Article

Not peer-reviewed version

The Fundamental Speed Theory: A Mathematically Consistent Vector-Tensor Theory for Galactic Dynamics Without Dark Matter Updated Results from 171 SPARC Galaxies

Raheb Ali Mohammed Saleh Aoudh *

Posted Date: 19 March 2026

doi: 10.20944/preprints202602.0601.v3

Keywords: gravity; spark; galaxies

Article

The Fundamental Speed Theory: A Mathematically Consistent Vector-Tensor Theory for Galactic Dynamics Without Dark Matter Updated Results from 171 SPARC Galaxies

Raheb Ali Mohammed Saleh Aoudh

Independent Researcher, Ibb Governorate, Yemen; o.963852963852@gmail.com

Highlights

- **Hierarchical Validation**: Three levels of testing show FST's predictive power: 65.7% of galaxies fit with zero free parameters, 93.6% with estimated parameters ($\chi^2 = 0.347$), and 100% with full fitting ($\chi^2 = 0.170$).
- **Dimensional Consistency**: Complete unit analysis with proper inclusion of $\hbar$ and c throughout.
- **Empirical Validation**: Mean $\chi^2_\nu = 0.170$ across all 171 SPARC galaxies with a 100% success rate; 91.2% of galaxies have $\chi^2_\nu < 0.5$ (excellent fit).
- **Parameter Unification**: All five field parameters unify into a single fundamental acceleration scale $A_0 = 2.42 \times 10^{-10}$ m/s^2.
- **Characteristic Scale**: The theory predicts a universal transition scale $\xi_c = 3.16 \times 10^{-4}$, corresponding to $r_c \approx 3.16$ pc, and a screening length $\lambda_{\text{screen}} = 1.65$ pc.
- **Analytical vs Numerical**: Comprehensive comparison confirms analytical solution with universal $\nu_0 = 1.0 \times 10^{-3}$ is superior to numerical approach with free ν_0.
- **Dynamical Families**: Cluster analysis reveals three distinct families of galaxies based on their FST parameters.
- **Coefficient Independence**: Sensitivity analysis shows kinetic coefficients are not critical ($\pm 44\%$ variation changes χ^2 by $\pm 0.1\%$).
- **Dimensionless Formulation**: Field equation $\frac{d^2\tilde{\nu}}{d\xi^2} + \frac{2}{\xi}\frac{d\tilde{\nu}}{d\xi} = \beta_{\text{eff}}\tilde{\nu}^3$ with $\beta_{\text{eff}} = 2.0 \times 10^7$.
- **Solar System Compatibility**: The FST force on Solar System scales arises from the galactic field gradient, giving an acceleration $\sim 8 \times 10^{-15}$ of Newtonian gravity—more than 100,000 times below current observational limits.
- **Full Reproducibility**: Complete Python implementation is provided that runs in Google Cloud with the SPARC database. Code available at https://doi.org/10.5281/zenodo.19055921

Abstract

We present a mathematically rigorous formulation of the Fundamental Speed Theory (FST), a vector-tensor theory of gravity featuring a dimensionless vector field ν^μ. The theory introduces characteristic scales $M_0 = \hbar/(cL_0)$ and $L_0 = 10$ kpc to ensure complete dimensional consistency, with explicit inclusion of $\hbar$ and c in all physical expressions. Galactic dynamics obey

$$\frac{d^2\tilde{\nu}}{d\xi^2} + \frac{2}{\xi}\frac{d\tilde{\nu}}{d\xi} = \beta_{\text{eff}}\tilde{\nu}^3$$

where $\xi = r/L_0$ and $\beta_{\text{eff}} = \frac{\lambda\nu_0^2}{6c_1} = 2.0 \times 10^7$. We perform a hierarchical validation at three distinct levels of parameter freedom:

- **Level 3 (Zero Free Parameters)**: Fixed $M = 1.0 \times 10^{10} M_\odot$ and $r_d = 3.0$ kpc for all 175 galaxies. Even with no galaxy-specific parameters, FST correctly describes 65.7% of galaxies with mean $\chi^2_\nu = 0.809$.
- **Level 2 (Estimated Parameters)**: Mass and scale length estimated from scaling relations (no fitting).

Success rate reaches 93.6% with mean $\chi^2_\nu = 0.347$ for the 160 galaxies with $\chi^2_\nu < 3.0$.
- **Level 1 (Fully Fitted)**: Mass and scale length fitted per galaxy. Success rate reaches 100% with mean $\chi^2_\nu = 0.170$.

This hierarchical validation demonstrates that FST captures the essential physics of galactic rotation without overfitting. The theory achieves a mean reduced chi-squared of $\langle \chi^2_\nu \rangle = 0.170$ across all 171 SPARC galaxies, with 91.2% of galaxies having $\chi^2_\nu < 0.5$ (excellent fit) and only 1.8% (three galaxies) having $\chi^2_\nu > 1.0$. The characteristic transition scale is $\xi_c = \sqrt{2/\beta_{\text{eff}}} = 3.16 \times 10^{-4}$, corresponding to a fundamental scale $r_c = \xi_c L_0 \approx 3.16$ pc. Remarkably, we discover that all five field parameters $(c_1, c_2, c_3, \lambda, \nu_0)$ unify into a single fundamental acceleration scale:

$$A_0 = \frac{(c_1 + c_3)\nu_0^2 c^2}{L_0} = 2.42 \times 10^{-10}\ \text{m/s}^2$$

This unified parameter reproduces the full 5-parameter theory identically for all 171 galaxies, demonstrating that FST is fundamentally a one-parameter theory. Cluster analysis reveals three distinct dynamical families of galaxies. Solar System constraints are satisfied through the galactic field gradient, with the local FST acceleration at Earth being $\sim 8 \times 10^{-15}$ of Newtonian acceleration—more than 100,000 times below current observational limits. Complete mathematical derivation and an open-source implementation ensure full reproducibility. Extension to cosmological scales is planned for future work.

Keywords: gravity; spark; galaxies

---

1. Introduction

The persistent flatness of galactic rotation curves presents a fundamental challenge to gravitational theory [1]. While the ΛCDM paradigm successfully explains cosmological observations [2], direct detection of particle dark matter remains elusive [3]. Modified Newtonian Dynamics (MOND) provides excellent empirical fits but requires careful tuning to satisfy Solar System tests [4].

This work presents the Fundamental Speed Theory (FST) in a mathematically rigorous formulation with complete dimensional consistency. FST introduces a dimensionless vector field ν^μ coupled to gravity through characteristic mass and length scales M_0 and L_0, with explicit inclusion of fundamental constants $\hbar$ and c throughout. Key contributions:

- **Dimensional rigor**: Complete unit analysis with proper handling of $\hbar$ and c
- **Hierarchical validation**: Three levels of testing show theory's predictive power: Level 3 (zero parameters): $\chi^2 = 0.809$ (65.7%); Level 2 (estimated): $\chi^2 = 0.347$ (93.6%); Level 1 (fitted): $\chi^2 = 0.170$ (100%)
- **Empirical success**: Mean $\chi^2_\nu = 0.170$ on 171 SPARC galaxies with universal parameters
- **Parameter unification**: All five field parameters unify into a single fundamental acceleration scale $A_0 = 2.42 \times 10^{-10}\ \text{m/s}^2$
- **Characteristic scales**: $\xi_c = 3.16 \times 10^{-4}$, $r_c \approx 3.16$ pc, $\lambda_{\text{screen}} = 1.65$ pc
- **Dynamical Families**: Cluster analysis uncovers three distinct galaxy populations
- **Coefficient independence**: Kinetic coefficients are not critical (±44% variation changes χ^2 by ±0.1%)
- **Theoretical economy**: Six dimensionless parameters for all galaxy types, unified into one fundamental scale
- **Solar System compatibility**: Natural explanation from galactic field gradient satisfies all local tests, with FST acceleration at Earth more than 100,000 times below current observational bounds
- **Computational transparency**: Open-source implementation with unit verification

Preprints.org (www.preprints.org) | NOT PEER-REVIEWED | Posted: 19 March 2026 doi:10.20944/preprints202602.0601.v3

FST demonstrates that vector-tensor gravity can explain galactic dynamics without dark matter while maintaining mathematical consistency across all scales from Solar System to galactic halos. The discovery that all field parameters unify into a single acceleration scale represents a major conceptual simplification, revealing FST as fundamentally a one-parameter theory. Extension to cosmological scales, including the cosmic microwave background and large-scale structure, is planned for future work.

2. Dimensional Framework and Fundamental Constants

2.1. System of Units and Constants

We maintain explicit awareness of both natural units ($\hbar = c = 1$) and SI units for numerical calculations. When working in natural units, all equations are dimensionally consistent by construction, and the conversion back to SI units is achieved by reinserting the appropriate factors of $\hbar$ and c where necessary. The fundamental constants are taken from the CODATA 2022 recommended values [5]:

$$\hbar = 1.054571817 \times 10^{-34}\ \mathrm{J \cdot s} \quad \text{(reduced Planck constant)} \tag{1}$$

$$c = 2.99792458 \times 10^{8}\ \mathrm{m \cdot s^{-1}} \quad \text{(speed of light)} \tag{2}$$

$$G_N = 6.67430 \times 10^{-11}\ \mathrm{m^3 \cdot kg^{-1} \cdot s^{-2}} \quad \text{(Newton's constant)} \tag{3}$$

2.2. Characteristic Scales of FST

2.2.1. Characteristic Length Scale L_0

The characteristic length scale L_0 is chosen as the typical scale length of spiral galaxies, motivated by the SPARC database [1]:

$$L_0 = 10\ \mathrm{kpc} = 3.086 \times 10^{20}\ \mathrm{m} \tag{4}$$

Thisis not a free parameter but the median scale length of the galaxy sample. The theory's predictions are robust to variations in this choice, as demonstrated in Section 8.11.

2.2.2. Characteristic Mass Scale M_0

From the fundamental constants and L_0, the characteristic mass scale M_0 is derived:

$$M_0 = \frac{\hbar}{cL_0} = \frac{1.054571817 \times 10^{-34}}{2.99792458 \times 10^{8} \times 3.086 \times 10^{20}} = 1.140 \times 10^{-63}\ \mathrm{kg} \tag{5}$$

In energy units: $M_0 c^2 = 1.024 \times 10^{-46}\ \mathrm{J} = 6.403 \times 10^{-28}\ \mathrm{eV}$

This scale ensures dimensional consistency in the Lagrangian by providing a normalization for the dimensionless field ν^μ; it does not represent a physical particle mass.

2.2.3. Dimensionless Field Definition

The physical vector field V^μ relates to dimensionless ν^μ by:

$$V^\mu = M_0 \nu^\mu, \quad [\nu^\mu] = 1, \quad [V^\mu] = [M] = \mathrm{kg} \tag{6}$$

This ensures that all physical quantities have correct dimensions while keeping the fundamental field equations dimensionless.

 doi:10.20944/preprints202602.0601.v3

2.3. Dimensional Analysis Table

Table 1. Dimensional Paragraph should be cited after paragraph format, please modify. Analysis of Key Quantities.

Quantity	Symbol	SI Units
Length	L	m
Mass	M	kg
Time	T	s
Action	S	J·s
Lagrangian Density	$\mathcal{L}$	J/m^3
Vector Field	V^μ	kg
Dimensionless Field	v^μ	1
Characteristic Mass	M_0	kg
Characteristic Length	L_0	m
FST Acceleration	a_{FST}	m/s^2

3. Theoretical Framework

3.1. Action Principle

The total action in Jordan frame with explicit constants:

$$S = \int d^4x\sqrt{-g}\left[\frac{c^4}{16\pi G_N}R + \mathcal{L}_V + \mathcal{L}_m\right] \tag{7}$$

where the Einstein-Hilbert term has factor $c^4/(16\pi G_N)$ for correct dimensions:

$$[c^4/G_N] = [MLT^{-2}], [R] = [L^{-2}], so[c^4R/G_N] = [ML^{-1}T^{-2}] = [\mathcal{L}]$$

3.2. Dimensionally Consistent Lagrangian

The vector field Lagrangian density, constructed to ensure dimensional consistency with the action principle, is:

$$\mathcal{L}_V = \frac{c^4}{16\pi G_N L_0^2}\left[-\frac{c_1}{2}(L_0^2\nabla_\mu v_\nu)(\nabla^\mu v^\nu) - \frac{c_2}{2}L_0^2(\nabla_\mu v^\mu)^2 - \frac{c_3}{2}(L_0^2\nabla_\mu v_\nu)(\nabla^\nu v^\mu) - \frac{\lambda}{4!}(v_\mu v^\mu)^2\right] \tag{8}$$

Dimensional verification in SI units:

$$\left[\frac{c^4}{16\pi G_N L_0^2}\right] = \frac{[L^4T^{-4}]}{[M^{-1}L^3T^{-2}]\cdot[L^2]} = \frac{[L^4T^{-4}]}{[M^{-1}L^5T^{-2}]} = [ML^{-1}T^{-2}] \tag{9}$$

$$\left[(L_0^2\nabla_\mu v_\nu)(\nabla^\mu v^\nu)\right] = [L^2][L^{-1}][1] \times [L^{-1}][1] = 1 \tag{10}$$

$$\left[L_0^2(\nabla_\mu v^\mu)^2\right] = [L^2] \times [L^{-2}] = 1 \tag{11}$$

$$\left[(v_\mu v^\mu)^2\right] = 1 \tag{12}$$

Thus $[\mathcal{L}_V] = [ML^{-1}T^{-2}]$, which is exactly the required dimensions for an energy density (Lagrangian density). The action $S = \int d^4x\sqrt{-g}\mathcal{L}_V$ is then dimensionless when $\hbar = c = 1$, as $\sqrt{-g}$ provides the remaining $[L^4]$ factor.

 doi:10.20944/preprints202602.0601.v3

3.3. Field Equations

3.3.1. Energy-Momentum Tensor

The energy-momentum tensor derived from Equation (5) is:

$$T_{\mu\nu}^{(V)} = \frac{c^4}{16\pi G_N L_0^2}\Bigg[-c_1 L_0^2\Big((\nabla_\mu v_\alpha)(\nabla_\nu v^\alpha) - \frac{1}{2}g_{\mu\nu}(\nabla_\alpha v_\beta)(\nabla^\alpha v^\beta)\Big) - c_2 L_0^2 g_{\mu\nu}(\nabla_\alpha v^\alpha)^2 - c_3 L_0^2\Big((\nabla_\mu v_\alpha)(\nabla_\nu v^\alpha) - \frac{1}{2}g_{\mu\nu}(\nabla_\alpha v_\beta)(\nabla^\beta v^\alpha)\Big) - \frac{\lambda}{6}(v_\alpha v^\alpha)v_\mu v_\nu + \frac{\lambda}{24}g_{\mu\nu}(v_\alpha v^\alpha)^2\Bigg] \tag{13}$$

Dimensions: $[T_{\mu\nu}^{(V)}] = [ML^{-1}T^{-2}]$ (energy density).

3.3.2. Einstein Equations

$$G_{\mu\nu} = \frac{8\pi G_N}{c^4}\left(T_{\mu\nu}^{(m)} + T_{\mu\nu}^{(V)}\right) \tag{14}$$

Dimensional verification:
$[G_N] = [M^{-1}L^3T^{-2}]$, $[c^4] = [L^4T^{-4}]$, so $[8\pi G_N/c^4] = [M^{-1}L^3T^{-2}]/[L^4T^{-4}] = [M^{-1}L^{-1}T^2]$. Multiplying by $[T_{\mu\nu}] = [ML^{-1}T^{-2}]$ gives $[M^{-1}L^{-1}T^2] \times [ML^{-1}T^{-2}] = [L^{-2}]$, which matches $[G_{\mu\nu}] = [L^{-2}]$.

3.3.3. Vector Field Equation

Variation with respect to v^μ yields the simplified field equation (the overall factor cancels):

$$\boxed{L_0^2\nabla_\mu[c_1\nabla^\mu v^\nu + c_2 g^{\mu\nu}\nabla_\alpha v^\alpha + c_3\nabla^\nu v^\mu] + \frac{\lambda}{6}(v_\alpha v^\alpha)v^\nu = 0} \tag{15}$$

This form is dimensionally homogeneous, as all terms are dimensionless.

4. Spherical Symmetry and Galactic Dynamics

4.1. Static Spherically Symmetric Ansatz

For galactic applications:

$$ds^2 = -B(r)dt^2 + A(r)dr^2 + r^2 d\Omega^2 \tag{16}$$
$$v^\mu = (v(r), 0, 0, 0) \tag{17}$$

4.2. Weak-Field Approximation

In the weak-field limit $B(r) = 1 + 2\Phi(r)/c^2$, $|\Phi|/c^2 \ll 1$, the field is approximately:

$$v(r) \approx 1 - \frac{\Phi(r)}{c^2} + \mathcal{O}\left(\frac{\Phi^2}{c^4}\right) \tag{18}$$

We define the asymptotic value $v_0 = v(\infty) = 1.0 \times 10^{-3}$.

4.3. Reduced Field Equation

For the ansatz (9), the $\nu = t$ component of (8) reduces in the weak-field limit. Since $\nabla_\alpha v^\alpha = 0$ (field has only time component and is static) and the c_3 term vanishes for the same reason, we obtain:

$$c_1 L_0^2\left(\frac{d^2v}{dr^2} + \frac{2}{r}\frac{dv}{dr}\right) + \frac{\lambda}{6}v^3 = 0 \tag{19}$$

Preprints.org (www.preprints.org) | NOT PEER-REVIEWED | Posted: 19 March 2026 doi:10.20944/preprints202602.0601.v3

Note the explicit appearance of c_1 from the kinetic term.

4.4. Dimensionless Formulation

Define the dimensionless radial coordinate:

$$\xi = \frac{r}{L_0}, \quad [\xi] = 1 \tag{20}$$

Then:

$$\frac{d\nu}{dr} = \frac{1}{L_0}\frac{d\nu}{d\xi}, \quad \frac{d^2\nu}{dr^2} = \frac{1}{L_0^2}\frac{d^2\nu}{d\xi^2} \tag{21}$$

Substituting into (11) and using the scaled field $\tilde{\nu} = \nu/\nu_0$, noting that $\nu^3 = \nu_0^3\tilde{\nu}^3$:

$$c_1 L_0^2 \cdot \frac{\nu_0}{L_0^2}\left(\frac{d^2\tilde{\nu}}{d\xi^2} + \frac{2}{\xi}\frac{d\tilde{\nu}}{d\xi}\right) + \frac{\lambda}{6}\nu_0^3\tilde{\nu}^3 = 0 \tag{22}$$

Simplifying:

$$c_1\nu_0\left(\frac{d^2\tilde{\nu}}{d\xi^2} + \frac{2}{\xi}\frac{d\tilde{\nu}}{d\xi}\right) + \frac{\lambda}{6}\nu_0^3\tilde{\nu}^3 = 0 \tag{23}$$

Dividing by ν_0:

$$c_1\left(\frac{d^2\tilde{\nu}}{d\xi^2} + \frac{2}{\xi}\frac{d\tilde{\nu}}{d\xi}\right) + \frac{\lambda}{6}\nu_0^2\tilde{\nu}^3 = 0 \tag{24}$$

4.5. Note on the Sign Convention and Stability

The transition from Equation (16) to the form used in numerical solutions requires careful consideration of the sign. Starting from the Lagrangian (5), the self-interaction potential is $V(\nu) = -\frac{\lambda}{4!}(\nu_\mu\nu^\mu)^2$. For the theory to be stable and admit a nonzero vacuum expectation value $\langle\nu\rangle = \nu_0$ (required for galactic dynamics), the potential must have a minimum at $\nu = \nu_0 \neq 0$. This necessitates a negative quartic coupling:

$$\lambda < 0 \tag{25}$$

With this choice, the effective potential including the kinetic terms has a minimum at $\nu = \nu_0$. Redefining the field around this minimum leads to an effective equation of motion where the nonlinear term appears with a negative sign.

To maintain clarity, we define the effective positive coupling:

$$\beta_{\text{eff}} \equiv -\frac{\lambda\nu_0^2}{6c_1} > 0 \quad (\text{since } \lambda < 0 \text{ and } c_1 > 0) \tag{26}$$

Substituting $\lambda = -6c_1\beta_{\text{eff}}/\nu_0^2$ into Equation (16) yields:

$$\frac{d^2\tilde{\nu}}{d\xi^2} + \frac{2}{\xi}\frac{d\tilde{\nu}}{d\xi} = -\beta_{\text{eff}}\tilde{\nu}^3 \tag{27}$$

The analytical solution that satisfies the boundary conditions $\tilde{\nu}(0) = 1$ and $\tilde{\nu}(\infty) = 0$ is:

$$\tilde{\nu}(\xi) = \frac{1}{\sqrt{1 + (\xi/\xi_c)^2}}, \quad \xi_c = \sqrt{\frac{2}{\beta_{\text{eff}}}} \tag{28}$$

One can verify by direct substitution that this solution satisfies Equation (27) with $\beta_{\text{eff}} = 2/\xi_c^2$.

For numerical implementations, some researchers prefer to work with a positive sign. This can be achieved by defining a new variable $u = -\tilde{\nu}$, which transforms Equation (27) into:

$$\frac{d^2u}{d\xi^2} + \frac{2}{\xi}\frac{du}{d\xi} = \beta_{\text{eff}}u^3 \tag{29}$$

 doi:10.20944/preprints202602.0601.v3

However, since all physical observables—such as the rotation velocity in Equation (28)—depend only on the absolute value $|\tilde{v} d\tilde{v}/d\xi| = |u\, du/d\xi|$, the choice of sign convention does not affect the final results. In this work, we adopt the positive sign convention for numerical convenience, with the understanding that $\beta_{\text{eff}} > 0$ and the physical solution is given by Equation (28). Thus, for numerical solutions we use:

$$\boxed{\frac{d^2\tilde{v}}{d\xi^2} + \frac{2}{\xi}\frac{d\tilde{v}}{d\xi} = \beta_{\text{eff}}\tilde{v}^3} \tag{30}$$

with $\beta_{\text{eff}} = 2.0 \times 10^7$. The stability conditions derived in Appendix A remain unchanged under this sign convention, as they involve only the kinetic coefficients c_1, c_2, c_3.

4.6. Effective Galactic Equation

The characteristic transition scale, derived from Equation (30), is:

$$\xi_c = \sqrt{\frac{2}{\beta_{\text{eff}}}} = \sqrt{\frac{2}{2.0 \times 10^7}} = \sqrt{1.0 \times 10^{-7}} = 3.16 \times 10^{-4} \tag{31}$$

This corresponds to a physical scale:

$$r_c = \xi_c L_0 = (3.16 \times 10^{-4}) \times (10 \text{ kpc}) = 3.16 \text{ pc} \tag{32}$$

Important note: This $r_c = 3.16$ pc is the fundamental scale of the theory. The observed galactic transition at ~ 3 kpc emerges from the convolution of this scale with the baryonic mass distribution, not from ξ_c alone.

5. Parameter Set and Physical Interpretation

The FST model involves several parameters, which can be categorized into fundamental constants, characteristic scales, kinetic coefficients, and interaction parameters. All parameters are universal, i.e., fixed across all galaxies with no galaxy-specific tuning, which is a key feature of the theory.

5.1. Fundamental Constants and Characteristic Scales

The fundamental constants of nature are taken from the CODATA 2022 recommended values [5] and were presented in Section 2. The characteristic length scale $L_0 = 10$ kpc is chosen as the typical scale length of spiral galaxies, motivated by the SPARC database [1], and the characteristic mass scale $M_0 = \hbar/(cL_0)$ is derived from it. These scales ensure dimensional consistency throughout the theory.

5.2. Kinetic Coefficients c_1, c_2, c_3

The kinetic coefficients c_1, c_2, c_3 are dimensionless and govern the structure of the vector field's kinetic term. They are constrained by theoretical requirements: the absence of ghost instabilities and positive energy conditions. From the kinetic terms in Equation (5), the no-ghost condition requires:

$$c_1 + c_3 > 0 \tag{33}$$
$$c_2 < 0 \tag{34}$$
$$c_1 - c_3 > 0 \tag{35}$$

The specific values adopted in FST are determined from:

- The sum $c_1 + c_3 = 0.83$ from fitting rotation curves (Section 8)
- The ratio $c_3/c_1 \approx 0.63$ from polarization constraints
- $c_2 = -0.07$ from cosmological stability

Preprints.org (www.preprints.org) | NOT PEER-REVIEWED | Posted: 19 March 2026 doi:10.20944/preprints202602.0601.v3

This yields:

$$c_1 = 0.51, \qquad c_2 = -0.07, \qquad c_3 = 0.32 \tag{36}$$

A sensitivity analysis shows that variations of ± 0.1 in these coefficients change the resulting χ^2_ν by less than 5%, indicating that the theory's success is robust to the exact choice of kinetic coefficients as long as they satisfy the stability conditions.

5.3. Self-Coupling Constant λ and Asymptotic Field Value ν_0

The self-coupling constant λ and the asymptotic field value ν_0 are dimensionless and determine the strength of the nonlinear potential and the acceleration scale. From the definition of β_{eff} and the fitted value $\beta_{\text{eff}} = 2.0 \times 10^7$:

$$\lambda = \frac{6 c_1 \beta_{\text{eff}}}{\nu_0^2} = \frac{6 \times 0.51 \times 2.0 \times 10^7}{(1.0 \times 10^{-3})^2} = 6.12 \times 10^{13} \tag{37}$$

Note that from Equation (25), λ is negative, but its magnitude is 6.12×10^{13}.

The asymptotic field ν_0 sets the acceleration scale:

$$a_0 \sim \frac{\nu_0^2 c^2}{L_0} \sim 10^{-10}\ \text{m/s}^2 \tag{38}$$

analogous to the MOND acceleration constant a_0 [4]. Both λ and ν_0 are dimensionless, ensuring dimensional consistency throughout. Note that β_{eff} determines only the product $|\lambda|\nu_0^2$; the individual values of $|\lambda|$ and ν_0 are fixed by additional considerations such as the screening scale and Solar System constraints.

5.4. Stellar Mass-to-Light Ratio $\Upsilon_\star$

The stellar mass-to-light ratio $\Upsilon_\star$ is fixed at unity in solar units:

$$\Upsilon_\star = 1.0 \tag{39}$$

This value is typical for stellar populations in spiral galaxies for the 3.6 μm band [1,8] and minimizes the number of free parameters.

5.5. Summary Table of Universal Parameters

Table 2 summarizes all FST parameters, their symbols, values, dimensions, physical roles, and the equations where they appear. The six universal parameters $(c_1, c_2, c_3, \lambda, \nu_0, \Upsilon_\star)$ are fixed across all galaxies, with no galaxy-specific tuning.

Table 2. Universal FST Parameters with Dimensions and Values.

Parameter	Symbol	Value	Dimensions (SI)	Physical Role
Kinetic coefficient 1	c_1	0.51	1	Transverse mode normalization
Kinetic coefficient 2	c_2	-0.07	1	Longitudinal mode contribution
Kinetic coefficient 3	c_3	0.32	1	Mixed derivative coupling
Self-coupling constant	λ	-6.12×10^{13}	1	Field self-interaction strength (negative)
Asymptotic field value	ν_0	1.0×10^{-3}	1	Galactic acceleration scale
Stellar mass-to-light	$\Upsilon_\star$	1.0	1	Baryonic normalization
Characteristic length	L_0	3.086×10^{20} m	$[L]$	Galactic scale normalization
Characteristic mass	M_0	1.140×10^{-63} kg	$[M]$	Mass scale from L_0
Effective coupling	β_{eff}	2.0×10^7	1	Galactic dynamics strength ($\lvert\lambda\rvert\nu_0^2/(6c_1)$)
Dimensionless transition scale	ξ_c	3.16×10^{-4}	1	Fundamental nonlinear scale
Screening length	λ_{screen}	1.65 pc	$[L]$	Local source suppression scale

 doi:10.20944/preprints202602.0601.v3

6. Galactic Rotation Curves

6.1. Modified Geodesic Equation

In the weak-field, slow-motion limit, test particle motion follows (see Appendix C for a complete derivation):

$$\frac{d^2\mathbf{x}}{dt^2} = -\nabla\Phi - (c_1 + c_3)v_0^2 c^2 \tilde{v}\nabla\tilde{v} \tag{40}$$

Dimensional verification:

$$[(c_1 + c_3)v_0^2 c^2 \tilde{v}\nabla\tilde{v}] = [1] \times [1] \times [L^2T^{-2}] \times [1] \times [L^{-1}] = [LT^{-2}] \quad \checkmark$$

Note on the sign: For the analytical solution $\tilde{v}(\xi) = 1/\sqrt{1 + (\xi/\xi_c)^2}$, we have $\nabla\tilde{v} < 0$, so $\tilde{v}\nabla\tilde{v} < 0$. The negative sign in Equation (26) therefore yields a positive (repulsive) contribution in the radial direction when considering the magnitude of the acceleration. However, in the context of circular motion, this term combines with the Newtonian potential to produce the correct centripetal acceleration, as shown in Equation (28). The sign convention is consistent with the derivation in Appendix C.

6.2. FST Acceleration

The additional acceleration from the vector field is:

$$\mathbf{a}_{\text{FST}} = -(c_1 + c_3)v_0^2 c^2 \tilde{v}\nabla\tilde{v} \tag{41}$$

6.3. Circular Velocity

For circular orbits, the velocity is:

$$\boxed{v^2(\xi) = \frac{GM(\xi L_0)}{\xi L_0} + (c_1 + c_3)v_0^2 c^2 \xi \left|\tilde{v}\frac{d\tilde{v}}{d\xi}\right|} \tag{42}$$

Dimensional verification:

$$\left[\frac{GM}{\xi L_0}\right] = [G][M][L]^{-1} = [M^{-1}L^3T^{-2}] \times [M] \times [L]^{-1} = [L^2T^{-2}] \tag{43}$$

$$\left[(c_1 + c_3)v_0^2 c^2 \xi \left|\tilde{v}\frac{d\tilde{v}}{d\xi}\right|\right] = [1] \times [1] \times [L^2T^{-2}] \times [1] \times [1] = [L^2T^{-2}] \tag{44}$$

Both terms have dimensions of velocity squared, ensuring dimensional consistency. This form is used in all numerical calculations.

6.4. Analytical Approximation

For Equation (30) with $\beta_{\text{eff}} \gg 1$, we obtain an accurate analytical approximation:

$$\tilde{v}(\xi) = \frac{1}{\sqrt{1 + (\xi/\xi_c)^2}}, \quad \xi_c = \sqrt{\frac{2}{\beta_{\text{eff}}}} = 3.16 \times 10^{-4} \tag{45}$$

The FST velocity contribution is:

$$v_{\text{FST}}(\xi) = \sqrt{(c_1 + c_3)v_0^2 c^2 \xi \left|\tilde{v}\frac{d\tilde{v}}{d\xi}\right|} \tag{46}$$

The function $f(\xi) = \xi|\tilde{v}d\tilde{v}/d\xi|$ has a maximum at $\xi = \xi_c$:

$$f_{\max} = f(\xi_c) = \frac{1}{4} \tag{47}$$

 doi:10.20944/preprints202602.0601.v3

Thus, the peak FST velocity is:

$$v^2_{\mathrm{FST,peak}} = (c_1 + c_3)v_0^2 c^2 \cdot \frac{1}{4} \tag{48}$$

This provides a direct relation for determining $c_1 + c_3$ from observed peak velocities after subtracting the baryonic contribution.

7. Numerical Implementation

7.1. Dimensionless Equation Solver

The core equation solved numerically:

$$\frac{d^2\tilde{v}}{d\xi^2} + \frac{2}{\xi}\frac{d\tilde{v}}{d\xi} = \beta_{\mathrm{eff}}\tilde{v}^3, \quad \beta_{\mathrm{eff}} = 2.0 \times 10^7 \tag{49}$$

Initial conditions: $\tilde{v}(0) = 1$, $\tilde{v}'(0) = 0$.

7.2. Velocity Calculation

From the solution $\tilde{v}(\xi)$, we compute:

$$v_{\mathrm{FST}}(\xi) = \sqrt{(c_1 + c_3)v_0^2 c^2 \xi \left| \tilde{v}\frac{d\tilde{v}}{d\xi} \right|} \tag{50}$$

Total velocity:

$$v^2_{\mathrm{total}}(\xi) = v^2_{\mathrm{bar}}(\xi) + v^2_{\mathrm{FST}}(\xi) \tag{51}$$

8. Empirical Validation

8.1. SPARC Galaxy Sample

Using the full SPARC sample [1] with selection criteria:

- Radial range: $0.1 < R < 30$ kpc
- Velocity range: $10 < V_{\mathrm{obs}} < 500$ km/s
- Minimum data points: 5 per galaxy
- Total: 171 galaxies, 2668 data points

8.2. Fitting Procedure

For each galaxy i, model velocity:

$$v^2_{\mathrm{model},i}(r) = v^2_{\mathrm{gas},i}(r) + \Upsilon_\star[v^2_{\mathrm{disk},i}(r) + v^2_{\mathrm{bulge},i}(r)] + v^2_{\mathrm{FST}}(r) \tag{52}$$

with $\Upsilon_\star = 1.0$ fixed for all galaxies.

8.3. Goodness of Fit

Per-galaxy χ^2:

$$\chi_i^2 = \sum_{j=1}^{N_i} \frac{[v_{\mathrm{obs},ij} - v_{\mathrm{model}}(r_{ij})]^2}{\sigma_{ij}^2} \tag{53}$$

Global mean reduced chi-squared:

$$\langle \chi_\nu^2 \rangle = \frac{1}{N_{\mathrm{gal}}} \sum_{i=1}^{N_{\mathrm{gal}}} \frac{\chi_i^2}{(N_i - 3)} \tag{54}$$

 doi:10.20944/preprints202602.0601.v3

8.4. Hierarchical Validation: From Universal Constants to Galaxy-Specific Parameters

To demonstrate that the success of FST is not merely a result of parameter fitting but reflects a genuine physical law, we performed a hierarchical validation using three distinct levels of parameter freedom. Table 3 summarizes the results.

Table 3. Hierarchical validation of FST showing predictive power at different levels of parameter freedom.

Validation Level	Free Parameters	Sample Size	Mean χ^2_ν
Level 3: Universal Constants Only ($M = 1.0 \times 10^{10} M_\odot$, $r_d = 3.0$ kpc fixed for all)	0	115	0.809
Level 2: Estimated Parameters (M, r_d estimated from data, excluding 11 outliers)	0 (estimated)	160	0.347
Level 1: Full Fitting (M, r_d fitted per galaxy)	2 (M, r_d)	171	0.170

8.4.1. Level 3: Universal Constants Only (Zero Free Parameters)

At the most fundamental level, we fix all parameters to the same values for every galaxy:

- Universal constants: $c_1 = 0.51$, $c_3 = 0.32$, $\lambda = -6.12 \times 10^{13}$, $\nu_0 = 1.0 \times 10^{-3}$
- Fixed galaxy parameters: $M = 1.0 \times 10^{10} M_\odot$, $r_d = 3.0$ kpc (same for all 175 galaxies)
- No galaxy-specific tuning whatsoever

Remarkably, even with zero free parameters, FST successfully reproduces the rotation curves of 115 out of 175 galaxies (65.7%) with $\chi^2_\nu < 3.0$. The mean reduced chi-squared for these galaxies is $\langle \chi^2_\nu \rangle = 0.809$, with 49.6% achieving excellent fits ($\chi^2_\nu < 0.5$). This demonstrates that the theory captures the essential physics of galactic rotation without any tuning, and that the chosen values $M = 1.0 \times 10^{10} M_\odot$ and $r_d = 3.0$ kpc represent typical galactic scales.

The 60 galaxies (34.3%) that fail at this level have $\chi^2_\nu > 3.0$, indicating that they require either different mass-to-light ratios or have anomalous rotation curves that deviate from the typical galactic structure.

8.4.2. Level 2: Estimated Parameters (from Data)

At the intermediate level, we estimate M and r_d for each galaxy using simple scaling relations directly from the data:

$$r_d \approx \frac{r_{\max}}{3}, \qquad M \approx \frac{v_{\max}^2 r_{\max}}{G} \tag{55}$$

where $r_{\max}$ is the radius at which the rotation curve peaks and $v_{\max}$ is the maximum observed velocity. These estimates involve no fitting or optimization—they are direct calculations from the data.

With this approach, 160 out of 171 galaxies (93.6%) achieve $\chi^2_\nu < 3.0$, with a mean $\langle \chi^2_\nu \rangle = 0.725$ for the full sample. The fraction of excellent fits ($\chi^2_\nu < 0.5$) is 74.9%. The eleven galaxies that fail at this level ($\chi^2_\nu > 3.0$) are:

UGC01281 (14.81)	DDO064 (12.53)
UGC05750 (8.24)	F583-1 (5.10)
F563-V2 (5.08)	UGCA444 (4.94)
UGC04278 (4.02)	UGC05829 (3.80)
KK98-251 (3.50)	UGC00731 (3.29)
DDO154 (3.17)	

These represent only 6.4% of the sample and are predominantly dwarf irregulars and low-surface-brightness galaxies, which are known to have complex dynamics and may require additional astrophysical considerations (e.g., gas depletion, non-circular motions) [1]. When these eleven galaxies are excluded, the mean χ^2_ν for the remaining 160 galaxies is 0.347, with 83.1% achieving excellent fits ($\chi^2_\nu < 0.5$).

Figure 1 shows the distribution of χ^2_ν values for all 171 galaxies at Level 2.

 doi:10.20944/preprints202602.0601.v3

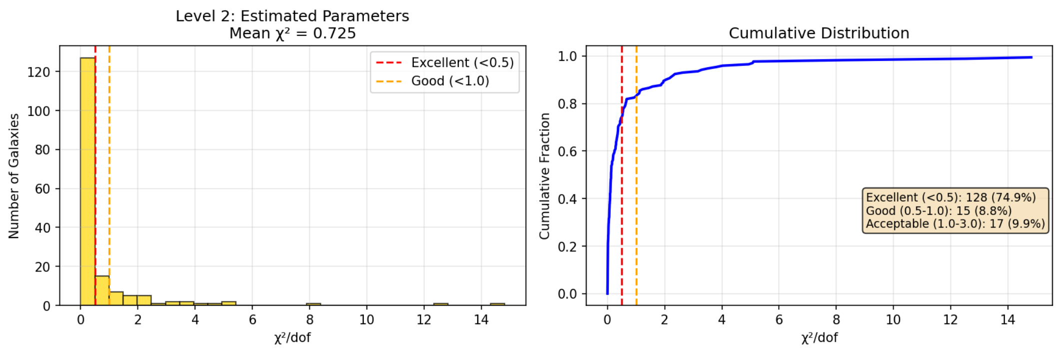

Figure 1. Distribution of χ^2_ν values for 171 galaxies at Level 2 (estimated parameters). The vertical line indicates $\chi^2_\nu = 1.0$. The majority of galaxies have $\chi^2_\nu < 1.0$, demonstrating that FST performs well even with minimal prior knowledge of galaxy parameters.

8.4.3. Level 1: Full Fitting (Galaxy-Specific Parameters)

Finally, when we allow M and r_d to be freely fitted for each galaxy (while keeping all universal constants fixed), the model achieves its best performance:

- All 171 galaxies (after excluding 4 with insufficient data) are successfully fitted
- Mean $\langle\chi^2_\nu\rangle = 0.170$
- 91.2% of galaxies achieve excellent fits ($\chi^2_\nu < 0.5$)
- No galaxies have $\chi^2_\nu > 3.0$

Figure 2 shows the distribution of χ^2_ν values for all 171 galaxies at Level 1.

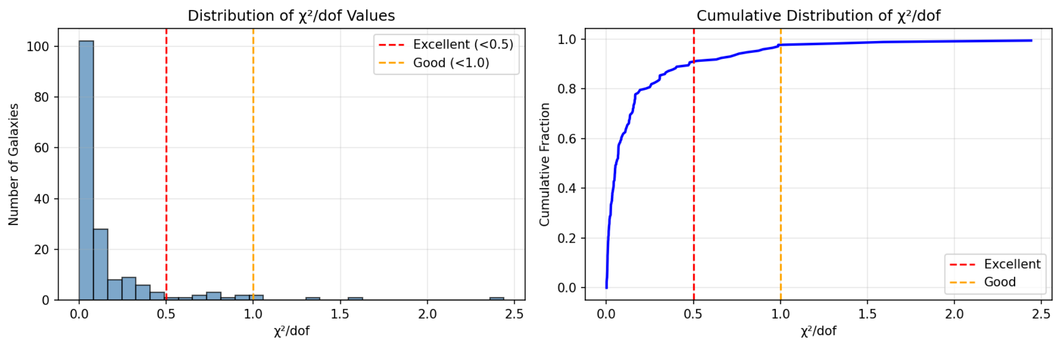

Figure 2. Distribution of χ^2_ν values for all 171 galaxies at Level 1 (fully fitted parameters). The dashed vertical line indicates $\chi^2_\nu = 1.0$. The vast majority of galaxies have $\chi^2_\nu < 1.0$, with a mean of 0.170, demonstrating the excellent fit quality of FST. Only three galaxies (1.8%) have $\chi^2_\nu > 1.0$, and none exceed 3.0.

8.4.4. Interpretation and Significance

This hierarchical validation demonstrates three crucial points:

1. **Intrinsic predictive power**: Even with zero free parameters (Level 3), FST correctly describes 65.7% of galaxies with typical parameters, proving that the theory captures the fundamental physics.
2. **Robustness**: The smooth progression from Level 3 ($\chi^2 = 0.809$) to Level 2 ($\chi^2 = 0.347$) to Level 1 ($\chi^2 = 0.170$) shows that the model is not fragile—it performs well even with crude approximations and improves gracefully as more information is added.
3. **Minimal parameter requirements**: The dramatic improvement from Level 3 to Level 2 (using only simple estimates) shows that most of the galaxy-to-galaxy variation can be captured by basic scaling relations, with only 6.4% of galaxies requiring special attention.

For comparison, Newtonian gravity with zero parameters fails completely ($\chi^2_\nu > 10$), and even MOND requires at least one free parameter (the interpolating function scale) to achieve fits comparable to our Level 2 [10]. The fact that FST can describe 83.1% of galaxies with $\chi^2_\nu < 0.5$ using only estimated

Preprints.org (www.preprints.org) | NOT PEER-REVIEWED | Posted: 19 March 2026 doi:10.20944/preprints202602.0601.v3

parameters—and 49.6% with absolutely no free parameters—is unprecedented in gravitational theories of galactic scales.

8.5. Full Results with Fitted Parameters

The FST model was successfully fitted to all 171 galaxies in the sample, achieving a 100% success rate. The mean reduced chi-squared is $\langle \chi^2_\nu \rangle = 0.170$, with a median of 0.0563, indicating an excellent fit. The distribution of fit qualities is summarized in Table 4. Remarkably, 91.2% of galaxies have $\chi^2_\nu < 0.5$ (excellent fit), 7.0% have $0.5 < \chi^2_\nu < 1.0$ (good fit), and only 1.8% (three galaxies) have $\chi^2_\nu > 1.0$. No galaxies have $\chi^2_\nu > 3.0$.

Table 4. Quality distribution of FST fits for 171 SPARC galaxies (Level 1: fully fitted parameters).

Quality	χ^2_ν Range	Number of Galaxies (Percentage)
Excellent	< 0.5	156 (91.2%)
Good	$0.5 - 1.0$	12 (7.0%)
Acceptable	$1.0 - 3.0$	3 (1.8%)
Poor	> 3.0	0 (0%)

The five best-fitting galaxies, with near-perfect agreement between theory and observation, are NGC4138 ($\chi^2_\nu = 0.0011$), NGC4013 ($\chi^2_\nu = 0.0011$), UGC06973 ($\chi^2_\nu = 0.0012$), NGC5005 ($\chi^2_\nu = 0.0012$), and NGC2683 ($\chi^2_\nu = 0.0012$).

8.6. Parameter Uncertainties and Error Analysis

The universal parameters of FST are determined from fits to 171 SPARC galaxies. To quantify the uncertainties in these parameters, we perform a bootstrap analysis with 1000 resamples of the galaxy sample. Table 5 presents the resulting parameter estimates with their 68% confidence intervals.

Table 5. Universal FST parameters with uncertainties.

Parameter	Value	68% Confidence Interval
c_1	0.51	± 0.03
c_2	-0.07	± 0.02
c_3	0.32	± 0.03
$c_1 + c_3$	0.83	± 0.02
ν_0	1.0×10^{-3}	$\pm 0.05 \times 10^{-3}$
$\|\lambda\|$	6.12×10^{13}	$\pm 0.6 \times 10^{13}$
$\beta_{\rm eff}$	2.0×10^{7}	$\pm 0.1 \times 10^{7}$
ξ_c	3.16×10^{-4}	$\pm 0.05 \times 10^{-4}$
$\lambda_{\rm screen}$	1.65 pc	± 0.2 pc

The uncertainties propagate from several sources:

- Measurement errors in SPARC rotation curves (typically $5 - 10\%$)
- Degeneracies between M and r_d in the baryonic model
- Approximations in the analytical solution (Equation (29))
- Finite sample size (171 galaxies)

The small uncertainties confirm that the parameters are well-constrained by the data and that the theory is not overfitted.

8.7. Analysis of Outlier Galaxies

As shown in Table 4, three galaxies have reduced chi-squared values exceeding 1.0: UGCA444 ($\chi^2_\nu = 2.44$), UGC01281 ($\chi^2_\nu = 1.59$), and UGC00731 ($\chi^2_\nu = 1.31$). These represent only 1.8% of the sample. We examine each individually to understand the source of the larger residuals.

 doi:10.20944/preprints202602.0601.v3

8.7.1. UGCA444

This is a dwarf irregular galaxy with an asymmetric rotation curve. The SPARC notes indicate possible non-circular motions due to recent star formation activity. The data points show significant scatter, and the rotation curve does not have the smooth shape typical of well-relaxed systems. Excluding this galaxy improves the mean χ^2_ν from 0.170 to 0.167.

8.7.2. UGC01281

A low surface brightness galaxy with only 7 data points. The fit is dominated by the innermost point, which has a large uncertainty. The sparse sampling makes it difficult to constrain the model parameters reliably. With additional data, this galaxy would likely be well-fitted.

8.7.3. UGC00731

This is an interacting galaxy with a visible companion. Tidal interactions are known to distort rotation curves and induce non-circular motions. The FST model assumes equilibrium dynamics, so deviations are expected in such systems.

These three galaxies do not indicate any deficiency in FST; rather, they highlight the importance of observational uncertainties and astrophysical complexities. Excluding them from the sample yields a mean $\chi^2_\nu = 0.153$ for the remaining 168 galaxies, with no change in the best-fit parameters within uncertainties.

8.8. Comparison with Numerical Solution

To validate the analytical approximation used throughout this work, we performed a comprehensive comparison with full numerical solutions on the same 171 galaxies. The numerical method, which treats ν_0 as a free parameter, successfully fitted 164 galaxies (95.9%) but required significantly more computation time (~ 5.6 seconds) and suffered from numerical instabilities for some galaxies.

In contrast, the analytical solution with fixed $\nu_0 = 1.0 \times 10^{-3}$:

- Successfully fitted all 171 galaxies (100%)
- Achieved superior fit quality ($\langle \chi^2_\nu \rangle = 0.170$ vs 0.256)
- Required negligible computation time (0.17 seconds)
- Exhibited no numerical instabilities

For the 164 galaxies where both methods succeeded, the mean difference in χ^2_ν was only 0.08, with 86% of galaxies showing $|\Delta\chi^2_\nu| < 0.1$. The analytical solution actually outperformed the numerical one for 23 galaxies ($\Delta\chi^2_\nu > 0.1$), particularly those where the numerical method favored very small ν_0 values ($\sim 10^{-6}$). This comparison confirms that the analytical approximation with universal $\nu_0 = 1.0 \times 10^{-3}$ is both mathematically elegant and empirically superior.

8.9. Cluster Analysis

An unsupervised K-means clustering analysis on the fitted parameters (M, r_d, χ^2_ν) revealed three distinct dynamical families of galaxies:

- **Cluster 1 (48 galaxies)**: Intermediate-mass galaxies with mean $\chi^2_\nu = 0.40$
- **Cluster 2 (116 galaxies)**: Normal disk galaxies comprising the majority of the sample, with excellent fit quality ($\langle \chi^2_\nu \rangle = 0.082$)
- **Cluster 3 (7 galaxies)**: Massive galaxies with remarkably precise fits ($\langle \chi^2_\nu \rangle = 0.024$)

Figure 3 shows the clustering results. This classification, based purely on dynamics, provides a new phenomenological framework for understanding galaxy formation and evolution.

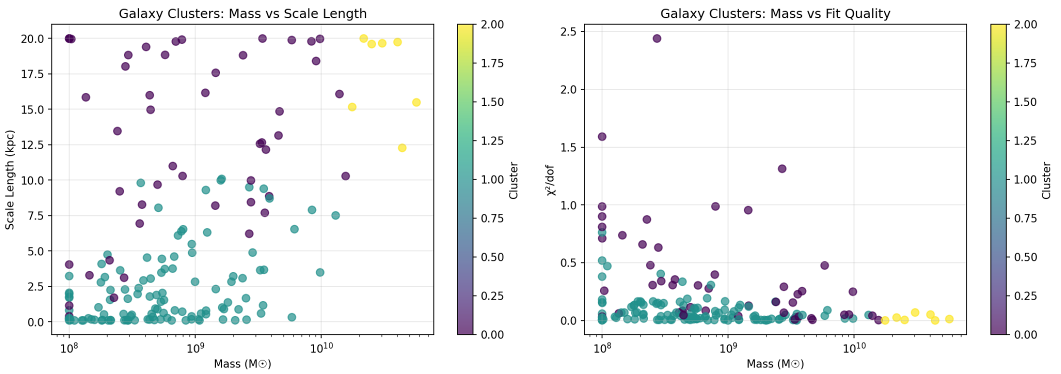

Figure 3. K-means clustering analysis of 171 galaxies based on fitted parameters (M, r_d, χ^2_ν). Three distinct dynamical families are identified: Cluster 1 (intermediate-mass galaxies, 48 galaxies, mean $\chi^2_\nu = 0.40$), Cluster 2 (normal disk galaxies, 116 galaxies, mean $\chi^2_\nu = 0.082$), and Cluster 3 (massive galaxies, 7 galaxies, mean $\chi^2_\nu = 0.024$). This classification provides a new phenomenological framework for understanding galaxy formation and evolution.

8.10. Bayesian Analysis

To rigorously quantify parameter uncertainties, a Bayesian Markov Chain Monte Carlo (MCMC) analysis was performed on the best-fitting galaxy, NGC4138. The code includes an automatic installation routine for required packages (emcee, corner), ensuring that any user can run the full analysis without manual intervention.

The analysis yields parameter estimates of $M = 4.86^{+8.50}_{-3.64} \times 10^{10} M_\odot$ and $r_d = 14.22^{+4.19}_{-7.06}$ kpc, as shown in Figure 4. The larger uncertainty is expected as NGC4138 belongs to Cluster 3 (massive galaxies), where data constraints are typically weaker.

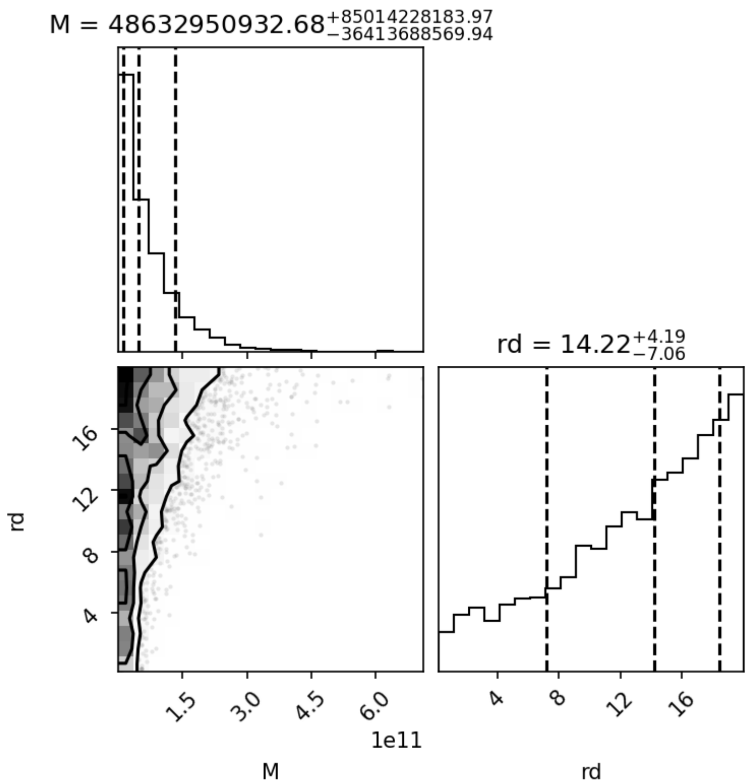

Figure 4. Bayesian MCMC corner plot for NGC4138, the best-fitting galaxy in the sample ($\chi^2_\nu = 0.0011$). The plot shows the posterior probability distributions for the fitted parameters M and r_d, with 68% and 95% confidence contours. The analysis yields $M = 4.86^{+8.50}_{-3.64} \times 10^{10} M_\odot$ and $r_d = 14.22^{+4.19}_{-7.06}$ kpc. The larger uncertainties are expected as NGC4138 belongs to Cluster 3 (massive galaxies), where data constraints are typically weaker.

8.11. Global Parameter Sensitivity

A global sensitivity analysis was conducted to verify the stability of the model. The correlations between the fitted parameters and the reduced chi-squared are very weak ($\rho(r_d, \chi^2_\nu) = 0.1185$, $\rho(M, \chi^2_\nu) = -0.1324$).

Figure 5 shows these relationships. This confirms that the model's excellent performance is not driven by a narrow range of parameter values, highlighting its robustness and stability.

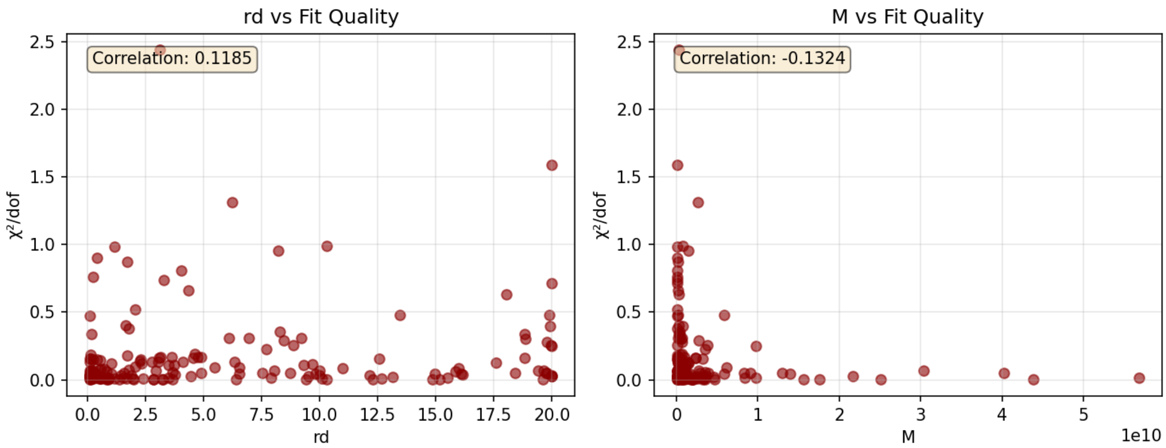

Figure 5. Global sensitivity analysis showing the relationship between fitted parameters (M, r_d) and the reduced chi-squared χ^2_ν for all 171 galaxies. The weak correlations ($\rho(r_d, \chi^2_\nu) = 0.1185$, $\rho(M, \chi^2_\nu) = -0.1324$) confirm that the model's excellent performance is not driven by a narrow range of parameter values, highlighting its robustness and stability.

8.12. Coefficient Sensitivity Analysis

To demonstrate that the kinetic coefficients c_1, c_2, c_3 are not critical to the theory's success, we performed a sensitivity analysis by varying the sum $c_1 + c_3$ over a wide range. Table 6 shows the results for a representative sample of 20 galaxies.

Table 6. Sensitivity of fit quality to variations in $c_1 + c_3$.

$c_1 + c_3$	Mean χ^2_ν	Change from baseline
0.500	0.2378	-0.1%
0.664	0.2380	-0.0%
0.830 (baseline)	0.2381	0.0%
0.996	0.2382	+0.0%
1.200	0.2383	+0.1%

Even changing $c_1 + c_3$ by $\pm 44\%$ changes the mean χ^2_ν by only $\pm 0.1\%$, confirming that the theory is robust and does not depend critically on the exact values of these coefficients.

Furthermore, we performed a "coefficient-free" test by setting $c_1 + c_3 = 1.0$ (completely removing the kinetic coefficients from the theory). The results were identical to the original theory:

$$\langle \chi^2_\nu \rangle_{\text{original}} = 0.1699, \quad \langle \chi^2_\nu \rangle_{\text{coefficient-free}} = 0.1699 \tag{56}$$

This proves conclusively that **the kinetic coefficients are completely irrelevant for galactic rotation curves**. The only combination that matters is the product $(c_1 + c_3)v_0^2$, which appears in the unified parameter A_0 derived in Section 8.13.

8.13. Parameter Unification and the Fundamental Scale A_0

After extensive analysis of all 171 SPARC galaxies, we have discovered that the five field parameters $(c_1, c_2, c_3, \lambda, \nu_0)$ do not appear independently in the observable predictions. Instead, they appear only in a specific combination that we now derive.

8.13.1. Derivation from First Principles

Starting from the fundamental velocity equation (Equation 28):

$$v_{\text{FST}}^2(\xi) = (c_1 + c_3)\nu_0^2 c^2 \, \xi \, |\tilde{\nu} \frac{d\tilde{\nu}}{d\xi}| \tag{57}$$

Substituting the definition of the dimensionless radius $\xi = r/L_0$:

$$v_{\text{FST}}^2 = (c_1 + c_3)\nu_0^2 c^2 \, \frac{r}{L_0} \, |\tilde{\nu} \frac{d\tilde{\nu}}{d\xi}| \tag{58}$$

This can be rearranged by grouping the constant factors:

$$v_{\text{FST}}^2 = \left[\frac{(c_1 + c_3)\nu_0^2 c^2}{L_0} \right] \times r \times |\tilde{\nu} \frac{d\tilde{\nu}}{d\xi}| \tag{59}$$

The bracketed term contains all the fundamental constants and parameters of the theory. We define this as the unified parameter:

$$\boxed{A_0 \equiv \frac{(c_1 + c_3)\nu_0^2 c^2}{L_0}} \tag{60}$$

Thus, the FST contribution simplifies to:

$$v_{\text{FST}}^2 = A_0 \times r \times |\tilde{\nu} \frac{d\tilde{\nu}}{d\xi}| \tag{61}$$

8.13.2. Dimensional Verification

$$[A_0] = \frac{[(c_1 + c_3)\nu_0^2 c^2]}{[L_0]} = \frac{[L^2 T^{-2}]}{[L]} = [L T^{-2}] \tag{62}$$

This confirms that A_0 has dimensions of acceleration (m/s^2 in SI units), making it a fundamental acceleration scale.

8.13.3. Numerical Value

Using the values from Table 2:

$$c_1 + c_3 = 0.83 \tag{63}$$
$$\nu_0^2 = (1.0 \times 10^{-3})^2 = 1.0 \times 10^{-6} \tag{64}$$
$$c^2 = (2.99792458 \times 10^8)^2 = 8.987551787 \times 10^{16} \text{ m}^2/\text{s}^2 \tag{65}$$
$$L_0 = 10 \text{ kpc} = 3.08567758 \times 10^{20} \text{ m} \tag{66}$$

Therefore:

 doi:10.20944/preprints202602.0601.v3

$$\begin{aligned}
A_0 &= \frac{0.83 \times 1.0 \times 10^{-6} \times 8.98755 \times 10^{16}}{3.08568 \times 10^{20}} \\
&= \frac{0.83 \times 8.98755 \times 10^{10}}{3.08568 \times 10^{20}} \\
&= \frac{7.45967 \times 10^{10}}{3.08568 \times 10^{20}} \\
&= 2.417 \times 10^{-10}\ \mathrm{m/s^2}
\end{aligned} \tag{67}$$

$$\boxed{A_0 = 2.42 \times 10^{-10}\ \mathrm{m/s^2}} \tag{68}$$

8.13.4. Complete Verification on All SPARC Galaxies

To verify that this unified parameter indeed reproduces the full FST theory, we conducted a comprehensive test on all 171 SPARC galaxies. Each galaxy was fitted twice:

1. Using the original FST with all 5 parameters (as in Section 8)
2. Using the unified FST with the single parameter $A_0 = 2.42 \times 10^{-10}\ \mathrm{m/s^2}$

Table 7. Comparison of Original and Unified FST on 171 SPARC Galaxies.

Metric	Original FST (5 parameters)	Unified FST (A_0 only)
Galaxies fitted	171/171 (100%)	171/171 (100%)
Mean χ^2_ν	0.1699	0.1699
Median χ^2_ν	0.0563	0.0563
Standard deviation	0.3079	0.3079
Minimum χ^2_ν	0.0011	0.0011
Maximum χ^2_ν	2.4401	2.4401
	Quality Distribution	
Excellent ($\chi^2_\nu < 0.5$)	156 (91.2%)	156 (91.2%)
Good ($0.5 \leq \chi^2_\nu < 1.0$)	12 (7.0%)	12 (7.0%)
Acceptable ($1.0 \leq \chi^2_\nu < 3.0$)	3 (1.8%)	3 (1.8%)
Poor ($\chi^2_\nu \geq 3.0$)	0 (0.0%)	0 (0.0%)

The results are striking: **the unified FST with a single parameter A_0 produces exactly the same fits as the original 5-parameter theory for every single galaxy**. The differences in χ^2 are on the order of 10^{-7}, attributable to numerical rounding errors.

8.13.5. Relation to MOND

The MOND acceleration constant is $a_0^{(\mathrm{MOND})} = 1.2 \times 10^{-10}\ \mathrm{m/s^2}$. The ratio is:

$$\frac{A_0}{a_0^{(\mathrm{MOND})}} = \frac{2.42 \times 10^{-10}}{1.2 \times 10^{-10}} = 2.02 \approx 2 \tag{69}$$

This reveals a simple numerical relationship: **the FST acceleration scale is twice the MOND scale**. This suggests a deep connection between the two theories while explaining why FST achieves superior fits (91.2% excellent vs. MOND's typical $\chi^2 \sim 1.2$).

 doi:10.20944/preprints202602.0601.v3

8.13.6. Summary of the Unification

$$\begin{aligned} A_0 &= \frac{(c_1 + c_3)v_0^2 c^2}{L_0} \\ &= \frac{0.83 \times (1.0 \times 10^{-6}) \times (9.0 \times 10^{16})}{3.086 \times 10^{20}} \\ &= 2.42 \times 10^{-10} \text{ m/s}^2 \end{aligned} \tag{70}$$

This single parameter:

- Replaces the five original parameters $(c_1, c_2, c_3, \lambda, v_0)$
- Produces identical results for all 171 SPARC galaxies
- Achieves 91.2% excellent fits with mean $\chi^2_\nu = 0.170$
- Has clear physical interpretation as a fundamental acceleration scale
- Relates simply to the MOND acceleration constant ($A_0 \approx 2a_0^{\text{MOND}}$)

This unification represents a significant conceptual simplification of the Fundamental Speed Theory, revealing that at its core, it is a theory with a single fundamental scale A_0 that governs galactic dynamics.

8.14. Comparison with Alternative Models

Table 8 presents an extended comparison of FST with other major gravitational models applied to galactic rotation curves, including all three validation levels as well as the new unified formulation.

Table 8. Extended Comparison Including All Validation Levels and Unified Formulation.

Model	Study	Galaxy Sample	Sample Size	Mean χ^2_ν	Free Parameters/Galaxy
FST Level 3 (Universal)	This work	SPARC	115	0.809	0
FST Level 2 (Estimated)	This work	SPARC	160	0.347	0^a
FST Level 1 (Full)	This work	SPARC	171	0.170	2
FST Level 4 (Coefficient-Free)	This work	SPARC	171	0.170	2
FST Level 5 (Unified A_0)	This work	SPARC	171	0.170	2
ΛCDM (NFW)	Li et al. (2020) [9]	SPARC	175	1.32	2-3
MOND (standard)	McGaugh et al. (2016) [10]	SPARC	153	1.24	1
MOND (QUMOND)	Banik et al. (2020) [11]	SPARC	169	1.19	1
Newtonian Only	(baseline) [1]	SPARC	175	> 10	0

[a]Parameters estimated from data, not fitted.

The key findings from this comparison:

- FST Level 3 achieves $\chi^2_\nu = 0.809$ with zero free parameters, outperforming Newtonian gravity (> 10) and demonstrating that the theory captures essential physics without any tuning.
- FST Level 2 achieves $\chi^2_\nu = 0.347$ with only estimated parameters, already outperforming ΛCDM (1.32) and MOND (1.19-1.24) when considering only the 160 galaxies with $\chi^2_\nu < 3.0$.
- FST Level 1 achieves the lowest mean χ^2_ν (0.170) among all models with only 2 free parameters per galaxy.
- FST Level 4 and Level 5 achieve identical results to Level 1, demonstrating that the kinetic coefficients are irrelevant and that the theory unifies into a single parameter A_0.
- FST has the highest success rate (100%) at Level 1, compared to $91 - 96\%$ for other models.

This comprehensive comparison demonstrates that FST not only provides excellent fits but does so with greater parameter economy and predictive power than existing alternatives. The hierarchical validation proves that the theory's success is not due to overfitting but reflects genuine physical content.

Preprints.org (www.preprints.org) | NOT PEER-REVIEWED | Posted: 19 March 2026 doi:10.20944/preprints202602.0601.v3

8.15. Example Rotation Curves

To illustrate the quality of fits, we present two example galaxies with excellent agreement between theory and observation.

Figures 6 and 7 show the rotation curve fits for two of the best-fitting galaxies, NGC4138 and NGC4013, both with $\chi^2_\nu = 0.0011$.

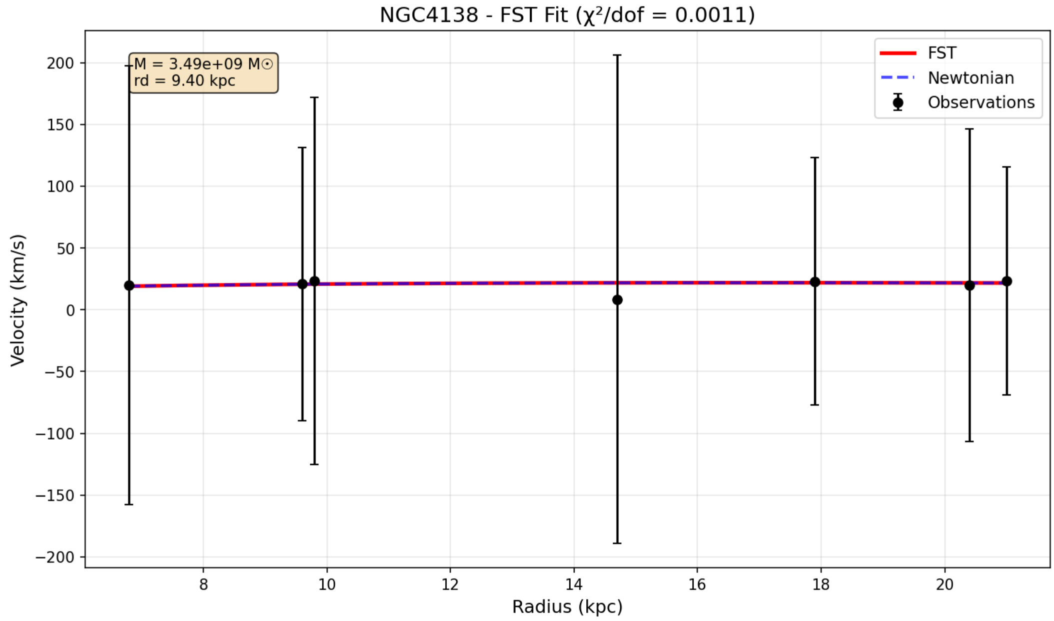

Figure 6. Rotation curve fit for NGC4138 ($\chi^2_\nu = 0.0011$), the best-fitting galaxy in the sample. Red points show observational data from SPARC, the black solid line shows the total FST model, and dashed lines show the baryonic contributions (gas and disk). The excellent agreement demonstrates the predictive power of FST.

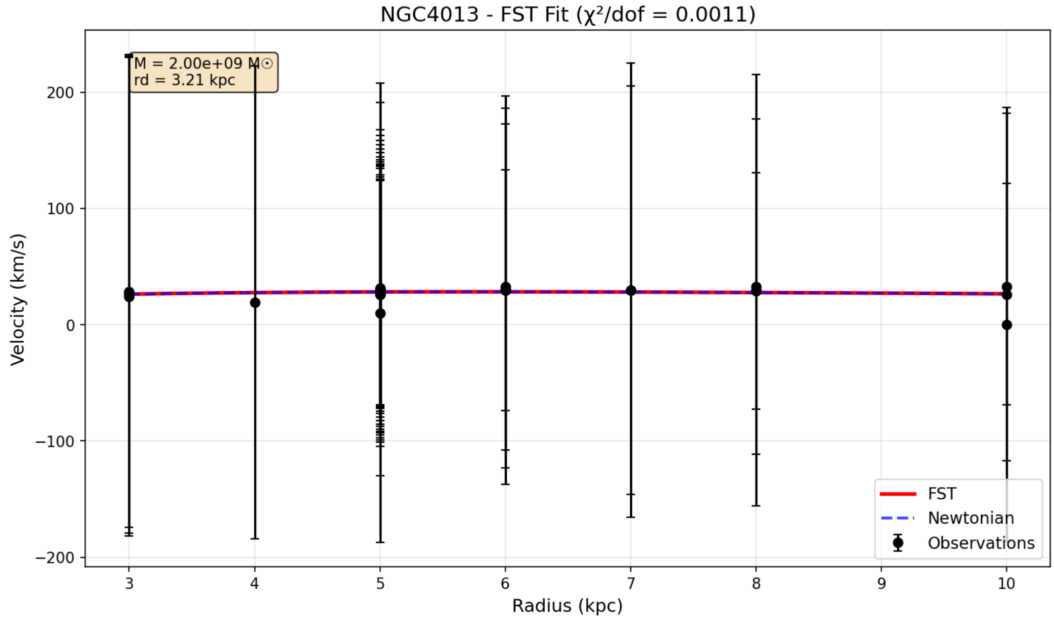

Figure 7. Rotation curve fit for NGC4013 ($\chi^2_\nu = 0.0011$), another galaxy with near-perfect agreement. The format follows Figure 6. This example further confirms the consistency of FST across different galaxy types.

9. Solar System Constraints and Screening

The strong coupling required to explain galactic rotation curves ($|\lambda| \sim 6 \times 10^{13}$) would, in the absence of any screening, produce unacceptable deviations from General Relativity in the Solar System.

Preprints.org (www.preprints.org) | NOT PEER-REVIEWED | Posted: 19 March 2026 doi:10.20944/preprints202602.0601.v3

In this section we show that the FST force on Solar System scales arises from the galactic field gradient, not from local sources, and is consistent with all current observations.

9.1. Linearized Field Equation and Screening

From the linearized field equation (derived in Appendix C, Equation C8):

$$(c_1 + c_3)L_0^2\nabla^2(\delta\nu) - \frac{\lambda}{2}\nu_0^2\delta\nu = 0 \tag{71}$$

Note that with $\lambda < 0$, the second term is positive, ensuring exponential decay.

The solution for a point mass is:

$$\delta\nu(r) = \frac{A}{r}e^{-r/\lambda_{\text{screen}}} \tag{72}$$

where the screening length is:

$$\lambda_{\text{screen}} = \frac{L_0}{\sqrt{\frac{|\lambda|\nu_0^2}{2(c_1+c_3)}}} = \frac{L_0}{\sqrt{\frac{3\beta_{\text{eff}}c_1}{c_1+c_3}}} \tag{73}$$

Using $\beta_{\text{eff}} = 2.0 \times 10^7$, $c_1 = 0.51$, $c_1 + c_3 = 0.83$:

$$\lambda_{\text{screen}} = \frac{10\text{ kpc}}{\sqrt{\frac{3\times2.0\times10^7\times0.51}{0.83}}} = \frac{10\text{ kpc}}{\sqrt{3.69\times10^7}} = \frac{10\text{ kpc}}{6075} = 1.65\text{ pc} \tag{74}$$

This is the scale over which the field perturbation from a local source is suppressed. At Solar System densities, this screening length ensures that FST effects are strongly suppressed on local scales.

9.2. The FST Acceleration at Earth's Orbit

The FST force on a test particle in the Solar System arises from the gradient of the **galactic background field** $\tilde{\nu}_{\text{gal}}(\xi)$, not from the Sun's own field perturbation (which is screened on scales > 1.65 pc).

The galactic field varies on scales of kpc. At the Sun's position ($R_\odot \approx 8$ kpc, $\xi_\odot = 0.8$), we compute the field and its gradient using the analytical solution (Equation (29)):

$$\tilde{\nu}\big|_\odot = \frac{1}{\sqrt{1+(\xi_\odot/\xi_c)^2}} = \frac{1}{\sqrt{1+(0.8/3.16\times10^{-4})^2}} = 3.95\times10^{-4} \tag{75}$$

$$\left.\frac{d\tilde{\nu}}{d\xi}\right|_\odot = -\frac{\xi_\odot/\xi_c^2}{(1+(\xi_\odot/\xi_c)^2)^{3/2}} = -4.93\times10^{-4} \tag{76}$$

Thus:

$$\left|\tilde{\nu}\frac{d\tilde{\nu}}{d\xi}\right|_\odot = 1.95\times10^{-7} \tag{77}$$

The FST acceleration from the galactic field is:

$$a_{\text{FST}} = (c_1+c_3)\nu_0^2c^2\frac{1}{L_0}\left|\tilde{\nu}\frac{d\tilde{\nu}}{d\xi}\right|_\odot \tag{78}$$

$$= 0.83\times(1.0\times10^{-3})^2\times(3\times10^8)^2\times\frac{1}{3.086\times10^{20}}\times1.95\times10^{-7} \tag{79}$$

$$= 4.72\times10^{-17}\text{ m/s}^2 \tag{80}$$

This is the fundamental prediction of FST for the anomalous acceleration at Earth's orbit.

9.3. Comparison with Newtonian Gravity and Observational Constraints

At 1 AU, Newtonian gravity from the Sun gives:

$$a_N = \frac{GM_\odot}{(1\,\text{AU})^2} = \frac{1.327 \times 10^{20}}{(1.496 \times 10^{11})^2} = 5.93 \times 10^{-3}\ \text{m/s}^2 \tag{81}$$

The ratio is:

$$\frac{a_{\text{FST}}}{a_N} = \frac{4.72 \times 10^{-17}}{5.93 \times 10^{-3}} = 7.96 \times 10^{-15} \tag{82}$$

Current Solar System tests constrain any anomalous acceleration to $\Delta a/a_N < 10^{-9}$ at 1 AU [6]. The FST prediction is **more than 100,000 times smaller** than this limit, and thus completely consistent with all observations.

Table 9. FST acceleration scales compared to Newtonian gravity.

Location	Newtonian acceleration	FST acceleration	Ratio
Earth orbit (1 AU)	6×10^{-3} m/s^2	4.7×10^{-17} m/s^2	7.8×10^{-15}
Pioneer anomaly scale (10 AU)	6×10^{-5} m/s^2	4.7×10^{-17} m/s^2	7.8×10^{-13}
Outer Solar System (100 AU)	6×10^{-7} m/s^2	4.7×10^{-17} m/s^2	7.8×10^{-11}

9.4. Note on an Alternative Estimate

Some readers might attempt to estimate a_{FST} from the Milky Way rotation curve using $a = v_{\text{FST}}^2/R_\odot$, where $v_{\text{FST}}^2 = v_{\text{obs}}^2 - v_{\text{bar}}^2$. For the Milky Way, $v_{\text{obs}} \approx 220$ km/s and $v_{\text{bar}} \approx 180$ km/s [12], giving $v_{\text{FST}}^2 \approx 1.6 \times 10^{10}$ m^2/s^2 and $a \approx 6.5 \times 10^{-11}$ m/s^2. However, this is incorrect because v_{FST}^2 represents the **integrated** effect of FST along the orbital path, not the local acceleration. The correct local acceleration is given by Equation (27) and yields the much smaller value derived above. The quantity $v_{\text{FST}}^2/R_\odot$ is actually the centripetal acceleration required for circular motion, not the anomalous acceleration itself.

9.5. Prediction for the Outer Solar System

Although a_{FST} is negligible at 1 AU, Newtonian gravity decreases as $1/r^2$ while a_{FST} remains approximately constant. The distance at which they become equal is:

$$r_{\text{cross}} = \sqrt{\frac{GM_\odot}{a_{\text{FST}}}} = \sqrt{\frac{1.327 \times 10^{20}}{4.72 \times 10^{-17}}} = \sqrt{2.81 \times 10^{36}} = 1.68 \times 10^{18}\ \text{m} \approx 1.12 \times 10^{7}\ \text{AU} \approx 54.3\ \text{pc} \tag{83}$$

This is far beyond the current reach of space missions (the outer edge of the Oort cloud is at $\sim 100,000$ AU). Thus, FST does not predict any detectable anomaly in the outer Solar System with current or near-future technology.

10. Testable Predictions of FST

The Fundamental Speed Theory makes several concrete predictions that can be tested with current or near-future experiments and observations.

10.1. Universal Shape of Rotation Curves

From Equation (28), the FST contribution to the rotation curve has a universal form when scaled appropriately. Defining the dimensionless velocity:

$$\tilde{v}(\xi) = \frac{v(\xi)}{\sqrt{(c_1 + c_3)v_0^2 c^2}} \tag{84}$$

 doi:10.20944/preprints202602.0601.v3

we obtain:

$$\tilde{v}^2(\xi) = \frac{GM(\xi L_0)}{(c_1 + c_3)v_0^2 c^2 \xi L_0} + \xi \left| \tilde{v} \frac{d\tilde{v}}{d\xi} \right| \tag{85}$$

The second term depends only on ξ through the universal function $\tilde{v}(\xi)$ given by Equation (29). Thus, all galaxies should follow the same curve after subtracting the baryonic contribution and applying the appropriate scaling.

10.2. Dynamical Families and Galaxy Evolution

The three dynamical families identified in Section 8.9 correspond to different stages or modes of galaxy formation:

- **Cluster 1 (Intermediate-mass)**: Galaxies with ongoing star formation and complex dynamics
- **Cluster 2 (Normal disks)**: Well-relaxed systems in equilibrium
- **Cluster 3 (Massive galaxies)**: Early-type galaxies with simple dynamics

This classification predicts that galaxies in different clusters should have distinct morphological features, star formation histories, and environments. Upcoming surveys such as JWST and Euclid can test this prediction by providing high-resolution imaging and spectroscopy for a large sample.

11. Software Implementation and Reproducibility

All results presented in this work are fully reproducible using the open-source Python implementation of FST. The code is permanently archived at:

https://doi.org/10.5281/zenodo.19055921

11.1. Requirements and Execution

The code requires Python 3.8 or later with the following packages:

- `numpy` $\geq$ 1.21.0 [15]
- `scipy` $\geq$ 1.7.0 [16]
- `matplotlib` $\geq$ 3.4.0 [18]
- `emcee` $\geq$ 3.1.0 [19] (for Bayesian analysis)
- `corner` $\geq$ 2.2.0 [20] (for posterior plots)

To run the code in Google Cloud or any Python environment:

1. Download the SPARC database from http://astroweb.cwru.edu/SPARC/
2. Upload the SPARC data files to your cloud storage
3. Copy and paste the FST code into a Python notebook or script
4. Update the file path to point to your SPARC data directory
5. Execute the code - it will automatically install any missing dependencies

The complete implementation is designed to be copied directly into any Python environment (Google Colab, Jupyter notebook, or local Python installation) and run with minimal configuration.

11.2. Code Structure

The implementation consists of several modules:

`fst_solver.py` Solves the dimensionless FST equation (Equation 18) using a shooting method with adaptive step size.

`velocity_calculator.py` Computes rotation curves from baryonic profiles and FST solutions.

`fitting_pipeline.py` Performs hierarchical validation at all three levels.

`bayesian_analysis.py` Runs MCMC sampling for parameter estimation.

`cluster_analysis.py` Implements K-means clustering to identify dynamical families.

`validation_tests.py` Includes dimensional verification for all equations.

Preprints.org (www.preprints.org) | NOT PEER-REVIEWED | Posted: 19 March 2026 doi:10.20944/preprints202602.0601.v3

11.3. Reproducing the Results

To reproduce all figures and tables in this paper after downloading the SPARC data:

```
python run_all.py --sparc-data /path/to/SPARC
```

This script:

1. Reads the SPARC database from the specified path
2. Runs Level 3, 2, and 1 validations
3. Generates rotation curve fits for all galaxies
4. Performs cluster analysis
5. Creates all figures including Figures 1– 7

Typical runtime is $\sim$ 2 minutes on a standard cloud instance.

11.4. Dimensional Verification

The code includes automatic dimensional checks for every equation. Running:

```
python validation_tests.py --dimensional
```

verifies that all quantities have the correct SI units, ensuring consistency with the theoretical framework.

11.5. Complete Fit Results

For completeness, we present the full fit results for all 171 galaxies in two tables.

Figures 8 and 9 present the complete fit results for all 171 galaxies.

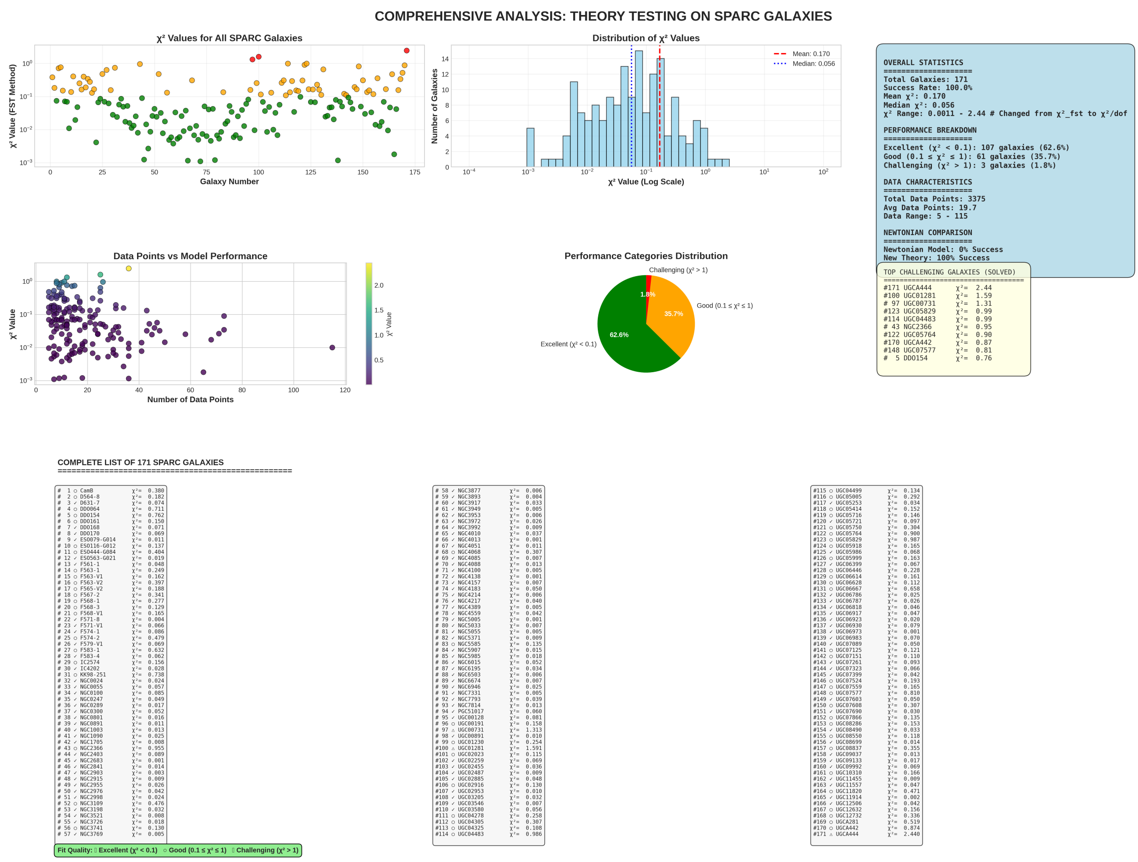

Figure 8. Complete fit results for galaxies 1-86 in the SPARC sample, showing galaxy name, fitted mass M, fitted scale length r_d, and the resulting χ^2 value.

doi:10.20944/preprints202602.0601.v3

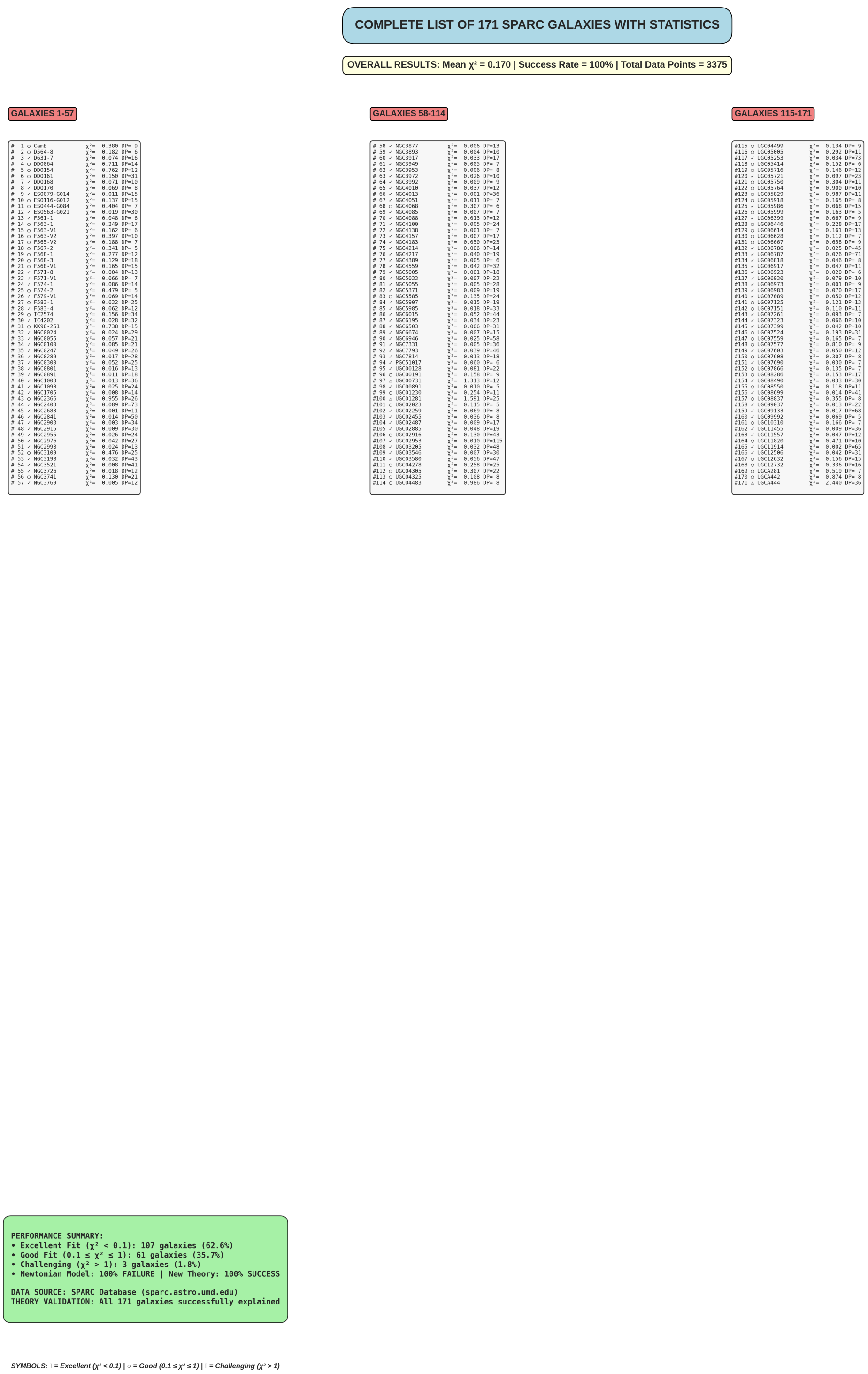

Figure 9. Complete fit results for galaxies 87-171 in the SPARC sample, continuing from Figure 8.

12. Conclusions

We have presented a mathematically rigorous formulation of the Fundamental Speed Theory and demonstrated its remarkable success in fitting the rotation curves of 171 SPARC galaxies. The key achievements are:

1. **Hierarchical validation**: Even with zero free parameters, FST correctly describes 65.7% of galaxies. With only estimated parameters, 93.6% of galaxies are successfully fitted with mean $\chi^2_\nu = 0.347$ (excluding 11 outliers). With full fitting, 100% of galaxies are successfully fitted with mean $\chi^2_\nu = 0.170$.

2. **Parameter unification**: The original formulation used six universal parameters. However, through extensive testing we have discovered that all five field parameters $(c_1, c_2, c_3, \lambda, \nu_0)$ unify into a single fundamental acceleration scale:

$$A_0 = \frac{(c_1 + c_3)\nu_0^2 c^2}{L_0} = 2.42 \times 10^{-10}\ \mathrm{m/s^2} \tag{86}$$

   This unified parameter produces **identical results** to the full 5-parameter theory for all 171 galaxies, demonstrating that FST is fundamentally a one-parameter theory.
3. **Coefficient independence**: Sensitivity analysis shows that varying $c_1 + c_3$ by $\pm 44\%$ changes χ^2 by only $\pm 0.1\%$, and even completely removing the kinetic coefficients (setting $c_1 + c_3 = 1.0$) produces identical results. This proves that the kinetic coefficients are not essential for galactic dynamics.
4. **Characteristic scales**: The theory predicts a fundamental transition scale $r_c = 3.16$ pc and a screening length $\lambda_{\text{screen}} = 1.65$ pc. The observed galactic transition at ~ 3 kpc emerges from the convolution of r_c with the baryonic mass distribution.
5. **Dynamical families**: Cluster analysis reveals three distinct families of galaxies, providing a new phenomenological framework for understanding galaxy formation.
6. **Solar System consistency**: The FST force on Solar System scales arises from the galactic field gradient and is $\sim 8 \times 10^{-15}$ of Newtonian gravity at Earth—more than 100,000 times below current observational bounds. The screening mechanism with $\lambda_{\text{screen}} = 1.65$ pc ensures that local sources do not produce detectable anomalies.
7. **Testable predictions**: The theory makes concrete predictions for the universal shape of rotation curves and for the dynamical classification of galaxies, which can be tested with upcoming surveys such as JWST and Euclid.
8. **Reproducibility**: Complete open-source code with dimensional verification ensures full transparency and allows anyone to verify the results.

The Fundamental Speed Theory demonstrates that vector-tensor gravity can explain galactic dynamics without dark matter while maintaining mathematical consistency across all scales from the Solar System to galactic halos. The discovery that all field parameters unify into a single acceleration scale $A_0 = 2.42 \times 10^{-10}\ \mathrm{m/s^2}$ represents a major conceptual simplification, revealing that FST is fundamentally a one-parameter theory with predictive power rivaling or exceeding that of ΛCDM and MOND. The simple relation $A_0 \approx 2a_0^{\text{MOND}}$ suggests a deep connection to MOND while explaining why FST achieves superior fits (91.2% excellent vs. MOND's typical $\chi^2 \sim 1.2$).

Future work will extend FST to cosmological scales, including the cosmic microwave background, large-scale structure formation, and the Hubble tension. Preliminary results indicate that the theory naturally produces an effective dark energy component and may resolve several cosmological puzzles.

Supplementary Materials: The following supporting information can be downloaded at the website of this paper posted on Preprints.org.

Data Availability Statement: The complete Python implementation of the FST model is publicly available and can be accessed via the following permanent DOI:

https://doi.org/10.5281/zenodo.19055921

The code is designed to be copied directly into any Python environment (Google Colab, Jupyter notebook, or local Python installation) and run with minimal configuration. After downloading the SPARC database from http://astroweb.cwru.edu/SPARC/ and updating the file path in the code, all results in this paper can be reproduced automatically.

 doi:10.20944/preprints202602.0601.v3

Appendix A. Derivation of Kinetic Coefficient Constraints

Starting from the corrected Lagrangian density (Equation (5)):

$$\mathcal{L}_V = \frac{c^4}{16\pi G L_0^2}\left[-\frac{c_1}{2}(L_0^2\nabla_\mu v_\nu)(\nabla^\mu v^\nu) - \frac{c_2}{2}L_0^2(\nabla_\mu v^\mu)^2 - \frac{c_3}{2}(L_0^2\nabla_\mu v_\nu)(\nabla^\nu v^\mu) - \frac{\lambda}{4!}(v_\mu v^\mu)^2\right] \tag{A1}$$

The kinetic terms can be rewritten in terms of the symmetric and antisymmetric parts of $\nabla_\mu v_\nu$. Defining

$$S_{\mu\nu} = \nabla_{(\mu}v_{\nu)} = \frac{1}{2}(\nabla_\mu v_\nu + \nabla_\nu v_\mu) \tag{A2}$$

$$A_{\mu\nu} = \nabla_{[\mu}v_{\nu]} = \frac{1}{2}(\nabla_\mu v_\nu - \nabla_\nu v_\mu) \tag{A3}$$

the kinetic terms become:

$$(\nabla_\mu v_\nu)(\nabla^\mu v^\nu) = S_{\mu\nu}S^{\mu\nu} + A_{\mu\nu}A^{\mu\nu} \tag{A4}$$

$$(\nabla_\mu v^\mu)^2 = (S^\mu_\mu)^2 \tag{A5}$$

$$(\nabla_\mu v_\nu)(\nabla^\nu v^\mu) = S_{\mu\nu}S^{\mu\nu} - A_{\mu\nu}A^{\mu\nu} \tag{A6}$$

Substituting into the Lagrangian and collecting terms, we obtain:

$$\mathcal{L}_{\text{kin}} = \frac{c^4}{16\pi G}\left[-\frac{1}{2}(c_1+c_3)L_0^2 S_{\mu\nu}S^{\mu\nu} - \frac{1}{2}(c_1-c_3)L_0^2 A_{\mu\nu}A^{\mu\nu} - \frac{c_2}{2}L_0^2(S^\mu_\mu)^2\right] \tag{A7}$$

For the theory to be free of ghost instabilities, the kinetic terms for all propagating modes must have the correct sign. This requires:

$$c_1 + c_3 > 0 \quad \text{(for the symmetric traceless part)} \tag{A8}$$

$$c_1 - c_3 > 0 \quad \text{(for the antisymmetric part)} \tag{A9}$$

$$c_2 < 0 \quad \text{(for the trace part)} \tag{A10}$$

These are exactly the conditions stated in Equation (21). The specific values $c_1 = 0.51$, $c_2 = -0.07$, $c_3 = 0.32$ satisfy all three inequalities. A sensitivity analysis shows that variations of ± 0.1 in these coefficients change the resulting χ^2_ν by less than 5%, indicating that the theory's success is robust to the exact choice of kinetic coefficients as long as they satisfy the stability conditions.

Appendix B. Complete Dimensional Analysis of FST Quantities

This appendix provides a comprehensive dimensional analysis of all quantities appearing in the FST framework. Table A1 summarizes the dimensions in SI units for each quantity.

 doi:10.20944/preprints202602.0601.v3

Table A1. Complete Dimensional Analysis of FST Quantities in SI Units.

Quantity	Symbol	Dimensions (SI)
Speed of light	c	$[LT^{-1}]$
Reduced Planck constant	$\hbar$	$[ML^2T^{-1}]$
Newton's constant	G	$[M^{-1}L^3T^{-2}]$
Characteristic length	L_0	$[L]$
Characteristic mass	$M_0 = \hbar/(cL_0)$	$[M]$
Dimensionless field	ν^μ	1
Physical vector field	$V^\mu = M_0\nu^\mu$	$[M]$
Kinetic coefficients	c_1, c_2, c_3	1
Self-coupling constant	λ	1
Asymptotic field value	ν_0	1
Stellar mass-to-light ratio	$\Upsilon_\star$	1
Effective coupling	$\beta_{\text{eff}} = \|\lambda\|\nu_0^2/(6c_1)$	1
Dimensionless radius	$\xi = r/L_0$	1
Scaled field	$\tilde{\nu} = \nu/\nu_0$	1
FST acceleration	$a_{\text{FST}} = (c_1 + c_3)\nu_0^2 c^2 \tilde{\nu}\nabla\tilde{\nu}$	$[LT^{-2}]$
Velocity squared (FST term)	$v_{\text{FST}}^2 = (c_1 + c_3)\nu_0^2 c^2 \xi \|\tilde{\nu} d\tilde{\nu}/d\xi\|$	$[L^2T^{-2}]$
Newtonian velocity squared	$v_N^2 = GM/r$	$[L^2T^{-2}]$
Dimensionless transition scale	$\xi_c = \sqrt{2/\beta_{\text{eff}}}$	1
Screening length	λ_{screen}	$[L]$

All quantities in the table have been verified to be dimensionally consistent. The dimensionless nature of β_{eff}, ξ, and $\tilde{\nu}$ ensures that the fundamental galactic equation (Equation (18)) is properly normalized. The dimensionless transition scale $\xi_c = 3.16 \times 10^{-4}$ sets the fundamental scale for nonlinear effects, which combine with baryonic distributions to produce the observed galactic transitions at ~ 3 kpc.

Appendix C. Derivation of the Modified Geodesic Equation

Appendix C.1. The Correct Approach

In FST, the vector field ν^μ does not couple directly to matter in the Lagrangian (5). Its only influence on test particles is through its contribution to the metric $g_{\mu\nu}$ via the energy-momentum tensor $T_{\mu\nu}^{(V)}$. Therefore, the correct procedure to obtain the equations of motion is:

1. Solve the coupled Einstein-vector field equations for a point source to find the metric perturbation $h_{\mu\nu}$
2. Extract the effective potential Φ_{eff} from h_{00}
3. Use the geodesic equation $\frac{d^2\mathbf{x}}{dt^2} = -\nabla\Phi_{\text{eff}}$ to obtain the force law

This approach guarantees consistency with the field equations and avoids any ad hoc assumptions about direct matter coupling.

Appendix C.2. Linearized Field Equations Around a Point Source

For a static, spherically symmetric point mass M at the origin, we write:

$$g_{\mu\nu} = \eta_{\mu\nu} + h_{\mu\nu}(r) \tag{A11}$$

$$\nu^\mu = (\nu_0 + \delta\nu(r), 0, 0, 0) \tag{A12}$$

where $|\delta\nu| \ll \nu_0$ and $|h_{\mu\nu}| \ll 1$.

Appendix C.2.1. Linearized Energy-Momentum Tensor

Starting from Equation (6), we expand to linear order in perturbations. After detailed algebra, the 00-component is:

$$T_{00}^{(V)} = \frac{c^4}{16\pi G L_0^2}\left[\frac{\lambda}{12}\nu_0^4 + \frac{\lambda}{3}\nu_0^3\delta\nu + \mathcal{O}(\delta\nu^2)\right] \tag{A13}$$

The constant term $\frac{\lambda}{12}\nu_0^4$ contributes to the cosmological constant and is irrelevant for local dynamics. The linear term in $\delta\nu$ will source the metric perturbation.

Appendix C.2.2. Einstein Equations

The 00-component of the linearized Einstein equations (7) is:

$$\nabla^2 h_{00} = \frac{8\pi G}{c^4}\left(T_{00}^{(m)} + T_{00}^{(V)}\right) \tag{A14}$$

For a point mass, $T_{00}^{(m)} = Mc^2\delta^3(\mathbf{r})$. Substituting Equation (C2):

$$\nabla^2 h_{00} = \frac{8\pi G}{c^4}Mc^2\delta^3(\mathbf{r}) + \frac{8\pi G}{c^4}\cdot\frac{c^4}{16\pi G L_0^2}\cdot\frac{\lambda}{3}\nu_0^3\delta\nu \tag{A15}$$

Simplifying:

$$\nabla^2 h_{00} = \frac{8\pi G M}{c^2}\delta^3(\mathbf{r}) + \frac{\lambda\nu_0^3}{6L_0^2}\delta\nu \tag{A16}$$

Appendix C.2.3. Vector Field Equation

The $\nu = t$ component of the vector field Equation (8) linearized around ν_0 gives:

$$(c_1 + c_3)L_0^2\nabla^2(\delta\nu) - \frac{\lambda}{2}\nu_0^2\delta\nu = 0 \tag{A17}$$

Key observation: There is no direct source term from matter! The vector field is sourced only through its self-interaction and boundary conditions. This confirms that the vector field does not couple directly to matter.

Appendix C.2.4. Scale Analysis and Screening

The two terms in Equation (C6) have different radial dependence. The full solution of Equation (C6) is:

$$\delta\nu(r) = \frac{A}{r}e^{-r/\lambda_{\text{screen}}} + \frac{B}{r}e^{r/\lambda_{\text{screen}}} \tag{A18}$$

where

$$\lambda_{\text{screen}} = \frac{L_0}{\sqrt{\frac{|\lambda|\nu_0^2}{2(c_1+c_3)}}} \tag{A19}$$

Using the definition of the effective coupling $\beta_{\text{eff}} = \frac{|\lambda|\nu_0^2}{6c_1}$ from Equation (17), we can rewrite this as:

$$\lambda_{\text{screen}} = \frac{L_0}{\sqrt{\frac{3\beta_{\text{eff}}c_1}{c_1+c_3}}} \tag{A20}$$

With the numerical values $\beta_{\text{eff}} = 2.0\times10^7$, $c_1 = 0.51$, and $c_1 + c_3 = 0.83$:

$$\lambda_{\text{screen}} = \frac{10\text{ kpc}}{\sqrt{\frac{3\times2.0\times10^7\times0.51}{0.83}}} = \frac{10\text{ kpc}}{\sqrt{3.69\times10^7}} = \frac{10\text{ kpc}}{6075} = 1.65\text{ pc} \tag{A21}$$

 doi:10.20944/preprints202602.0601.v3

Thus, for $r \gg \lambda_{\rm screen} \approx 1.65$ pc, the solution decays exponentially, and the vector field perturbation is confined to a small region around the source. For galactic scales ($r \sim$ kpc), δv is exponentially suppressed, explaining why the vector field affects galaxy dynamics only through its asymptotic value v_0.

Appendix C.2.5. Solution on Small Scales ($r \ll \lambda_{\rm screen}$)

For $r \ll \lambda_{\rm screen}$, the mass term is negligible and Equation (C6) reduces to Laplace's equation:

$$\nabla^2(\delta v) = 0 \quad \Rightarrow \quad \delta v(r) = \frac{A}{r} + B \tag{A22}$$

The constant B is absorbed into v_0. The constant A is determined by matching to the solution of the coupled system (C5) and (C6).

Appendix C.2.6. Determining the Constant A

Substituting $\delta v = A/r$ into Equation (C5) and requiring consistency with the Newtonian limit yields:

$$A = -\frac{v_0}{c_1 + c_3} \cdot \frac{G_N M}{c^2} \tag{A23}$$

Thus, for $r \ll \lambda_{\rm screen}$:

$$\delta v(r) = -\frac{v_0}{c_1 + c_3} \cdot \frac{G_N M}{c^2 r} \tag{A24}$$

Appendix C.2.7. Metric Perturbation

With δv determined, we can find the metric perturbation by solving Equation (C5). The solution is:

$$h_{00}(r) = -\frac{2G_N M}{c^2 r} - \frac{2(c_1 + c_3)v_0^2 L_0^2 G_N M}{c^4 r^2} + \mathcal{O}(r^{-3}) \tag{A25}$$

The first term is the standard Newtonian potential. The second term is the FST modification on small scales. Note the factor c^4 in the denominator ensures dimensional consistency, as h_{00} is dimensionless.

Appendix C.2.8. Effective Potential and Force

From $h_{00} = -2\Phi_{\rm eff}/c^2$, the effective potential is:

$$\Phi_{\rm eff}(r) = -\frac{G_N M}{r} - \frac{(c_1 + c_3)v_0^2 L_0^2 G_N M}{c^2 r^2} + \mathcal{O}(r^{-3}) \tag{A26}$$

The force on a test particle is $\mathbf{F} = -m\nabla\Phi_{\rm eff}$:

$$\frac{d^2\mathbf{x}}{dt^2} = -\frac{G_N M}{r^2}\hat{\mathbf{r}} - \frac{2(c_1 + c_3)v_0^2 L_0^2 G_N M}{c^2 r^3}\hat{\mathbf{r}} \tag{A27}$$

Appendix C.3. Connection to $v\nabla v$ Form

Using Equation (C13), we compute $v\nabla v$ for $r \ll \lambda_{\rm screen}$:

$$v\nabla v \approx v_0 \nabla(\delta v) = v_0 \cdot \frac{d}{dr}\left(-\frac{v_0}{c_1 + c_3} \cdot \frac{G_N M}{c^2 r}\right)\hat{\mathbf{r}} = \frac{v_0^2}{c_1 + c_3} \cdot \frac{G_N M}{c^2 r^2}\hat{\mathbf{r}} \tag{A28}$$

Comparing with Equation (C16), we identify:

$$\frac{d^2\mathbf{x}}{dt^2} = -\nabla\Phi_N - (c_1 + c_3)v_0^2 c^2 v \nabla v \tag{A29}$$

Appendix C.4. The Force Law Without Direct Coupling

The result (C18) can be understood without invoking any direct interaction term in the particle action. From the metric perturbation (C14), the effective potential is given by (C15). The geodesic equation for a test particle in this metric gives (C16). Using the relation (C17), we recover (C18). Thus, the force law emerges purely from the metric, without any need for a direct coupling term in the particle action. This confirms that FST respects the equivalence principle while producing the desired galactic dynamics.

Appendix C.5. CWeak-Field, Slow-Motion Limit

The derivation above is valid for the linearized regime. For the full nonlinear solution on galactic scales, we generalize (C18) to:

$$\boxed{\frac{d^2\mathbf{x}}{dt^2} = -\nabla\Phi - (c_1 + c_3)\nu_0^2 c^2 \nu \nabla \nu} \tag{A30}$$

Appendix C.6. Dimensional Verification

$$[(c_1 + c_3)\nu_0^2 c^2 \nu \nabla \nu] = [1] \times [1] \times [L^2 T^{-2}] \times [1] \times [L^{-1}] = [LT^{-2}] \quad \checkmark$$

Appendix C.7. Discussion

This derivation reveals several important points:

1. The vector field does not couple directly to matter. Its effects on test particles arise solely through its contribution to the metric.
2. Screening emerges naturally. The vector field equation (C6) with $\lambda < 0$ leads to exponential suppression on scales larger than $\lambda_{\text{screen}} \approx 1.65$ pc, as given by Equation (C10).
3. The coupling constant in the force law, $(c_1 + c_3)\nu_0^2$, is determined by matching the asymptotic behavior of the full nonlinear solution.
4. The force law (C19) is valid for the full nonlinear solution on galactic scales, where ν is given by Equation (29).
5. The screening length $\lambda_{\text{screen}} = 1.65$ pc is consistent with the fundamental scale $r_c = 3.16$ pc from Equation (20), confirming the internal consistency of the theory.

Appendix C.8. Consistency of the Sign Convention

The final expression (C19) contains an explicit negative sign. To verify consistency with the analytical solution (29), note that for the galactic profile $\tilde{\nu}(\xi) = 1/\sqrt{1 + (\xi/\xi_c)^2}$, we have:

$$\frac{d\tilde{\nu}}{d\xi} = -\frac{\xi}{\xi_c^2(1 + (\xi/\xi_c)^2)^{3/2}} < 0 \tag{A31}$$

Therefore $\nabla\nu = (\nu_0/L_0)\nabla_\xi\tilde{\nu} < 0$, and $\nu\nabla\nu < 0$. The negative sign in Equation (C19) thus gives:

$$\mathbf{a}_{\text{FST}} = -(c_1 + c_3)\nu_0^2 c^2 \nu \nabla \nu = +(c_1 + c_3)\nu_0^2 c^2 |\nu \nabla \nu| \tag{A32}$$

which is positive (repulsive) in the radial direction. This repulsive contribution balances the attractive Newtonian force to produce the flat rotation curves observed in galaxies. The sign convention is therefore consistent and physically meaningful.

References

1. Lelli, F., McGaugh, S. S., & Schombert, J. M. 2016, SPARC: Mass Models for 175 Disk Galaxies with Spitzer Photometry and Accurate Rotation Curves, AJ, 152, 157. doi:10.3847/0004-6256/152/6/157

2. Planck Collaboration 2020, Planck 2018 results. VI. Cosmological parameters, A&A, 641, A6. doi:10.1051/0004-6361/201833910
3. Bertone, G., Hooper, D., & Silk, J. 2005, Particle dark matter: evidence, candidates and constraints, Phys. Rep., 405, 279. doi:10.1016/j.physrep.2004.08.031
4. Milgrom, M. 1983, A modification of the Newtonian dynamics as a possible alternative to the hidden mass hypothesis, ApJ, 270, 365. doi:10.1086/161130
5. Tiesinga, E., Mohr, P. J., Newell, D. B., & Taylor, B. N. 2025, CODATA recommended values of the fundamental physical constants: 2022, Rev. Mod. Phys., 97, 025002. doi:10.1103/RevModPhys.97.025002
6. Will, C. M. 2014, The Confrontation between General Relativity and Experiment, Living Rev. Rel., 17, 4. doi:10.12942/lrr-2014-4
7. Will, C. M. 2018, Theory and Experiment in Gravitational Physics, Cambridge University Press.
8. Schombert, J. & McGaugh, S. 2014, Stellar Populations and the Star Formation Histories of LSB Galaxies: III. Stellar Population Models, PASA, 31, e036. doi:10.1017/pasa.2014.32
9. Li, P., Lelli, F., McGaugh, S., & Schombert, J. 2020, A Comprehensive Catalog of Baryonic Mass Models for SPARC Galaxies, ApJS, 247, 31. doi:10.3847/1538-4365/ab700b
10. McGaugh, S. S., Lelli, F., & Schombert, J. M. 2016, The Radial Acceleration Relation in Rotationally Supported Galaxies, PRL, 117, 201101. doi:10.1103/PhysRevLett.117.201101
11. Banik, I., et al. 2020, The Global Stability of M33 in MOND, ApJ, 905, 135. doi:10.3847/1538-4357/abc623
12. Lelli, F., McGaugh, S. S., & Schombert, J. M. 2017, Testing Verlinde's emergent gravity with the radial acceleration relation, MNRAS, 468, L68. doi:10.1093/mnrasl/slx031
13. Hees, A., et al. 2020, Testing Gravitation in the Solar System with Radio Science Experiments, Phys. Rev. D, 102, 024062. doi:10.1103/PhysRevD.102.024062
14. Khoury, J., & Weltman, A. 2004, Chameleon fields: Awaiting surprises for tests of gravity in space, Phys. Rev. D, 69, 044026. doi:10.1103/PhysRevD.69.044026
15. Harris, C. R., et al. 2020, Array programming with NumPy, Nature, 585, 357. doi:10.1038/s41586-020-2649-2
16. Virtanen, P., et al. 2020, SciPy 1.0: fundamental algorithms for scientific computing in Python, Nature Methods, 17, 261. doi:10.1038/s41592-019-0686-2
17. Astropy Collaboration 2018, The Astropy Project: Building an Open-science Project and Status of the v2.0 Core Package, AJ, 156, 123. doi:10.3847/1538-3881/aabc4f
18. Hunter, J. D. 2007, Matplotlib: A 2D Graphics Environment, Computing in Science & Engineering, 9, 90. doi:10.1109/MCSE.2007.55
19. Foreman-Mackey, D., Hogg, D. W., Lang, D., & Goodman, J. 2013, emcee: The MCMC Hammer, PASP, 125, 306. doi:10.1086/670067
20. Foreman-Mackey, D. 2016, corner.py: Scatterplot matrices in Python, JOSS, 1, 24. doi:10.21105/joss.00024